LUND UNIVERSITY

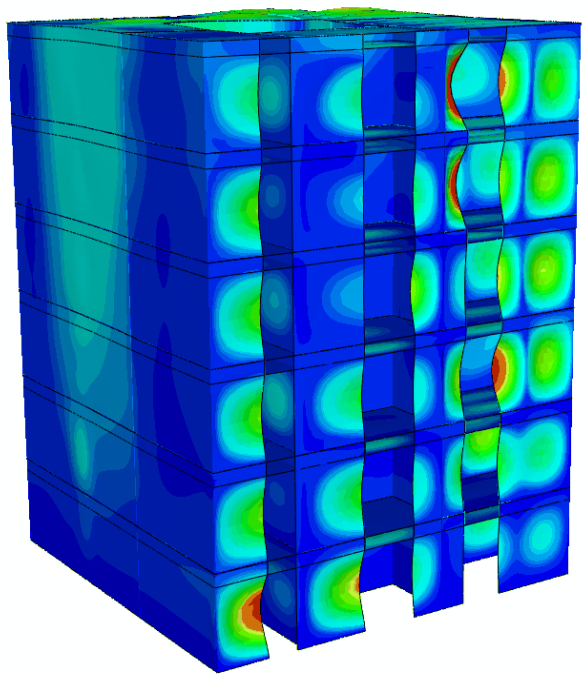

VIBRATIONS IN A SEVEN-STOREY WOOD BUILDING

LIVIA HOLTERMAN and ÅSA PETERSSON

Structural Mechanics

Master's Dissertation

Department of Construction Sciences
Structural Mechanics

ISRN LUTVDG/TVSM--08/5157--SE (1-72)
ISSN 0281-6679

VIBRATIONS IN A SEVEN-STOREY WOOD BUILDING

Master's Dissertation by

LIVIA HOLTERMAN and ÅSA PETERSSON

Supervisors:

Delphine Bard, Dr.Sc.,
Div. of Engineering Acoustics

Kent Persson, PhD,
Div. of Structural Mechanics

Examiner:

Göran Sandberg, Professor,
Div. of Structural Mechanics

Printed by KFS I Lund AB, Lund, Sweden, June, 2008.

For information, address:
Division of Structural Mechanics, LTH, Lund University, Box 118, SE-221 00 Lund, Sweden.
Homepage: http://www.byggmek.lth.se

Preface

This master thesis was carried out at the Division of Structural Mechanics at LTH, Lund University, Sweden, over a period from November 2007 to May 2008.

We would like to thank Ph.D. Kent Persson at the Division of Structural Mechanics for his great assistance during this project without which this thesis would not have been possible. A special thanks to Dr.Sc. Delphine Bard at the Division of Engineering Acoustics who during a long day at *Limnologen* showed us how vibration measurements are carried out. Moreover we would like to express our gratitude to the staff at the Division of Structural Mechanics that contributed with valuable suggestions along the way.

We would also like to thank our families and friends for supporting us and keeping up our good spirit.

Lund, May 2008

Livia Holterman and Åsa Petersson

Abstract

In 1994 the Swedish Construction Code, *BKR*, was changed from being based on material to being based on function. This permitted constructing multi-storey buildings with a bearing framework made of wood, which had been prohibited since the end of the 19th century. There is now a growing interest of using wood as a construction material. In Växjö four seven-storey buildings, *Limnologen*, are under construction, which at the moment are the highest wood buildings in Sweden. As wood in many ways is a new construction material there is a lot of research going on in order to build as good as possible. The main problems, when constructing in wood, are sound and vibrations because of the low weight of the material.

This thesis is part of a project at Växjö University examining step sounds and vibrations at *Limnologen*. The objective of our project was to investigate how mechanical vibrations are transmitted through the building at different storeys. The long term goal is to construct high buildings where residents are not disturbed by the noise or motion of their neighbors.

A FE-model of six storeys of the house was created with help of the finite element software *Abaqus*. It would be impossible to handle and perform vibration calculations on a detailed model of the building. Therefore a lot of simplifications were necessary. First of all detailed small scale FE-models of the main building parts (floor structure, ceiling and apartment separating wall) were produced and some analyses were conducted on them to find their normal, bending and torsion stiffness. The full-scale model was then composed of shells with the same stiffness. To variate the stiffness of the connections between walls and floor structures three different models were produced, one with fixed connections and two with weaker ones. Air was not included in the model. In the analyses a harmonic load of 700 N, approximately the weight of one person, was added at the same position on storey 2, 4 and 6, one at a time. A steady-state step was conducted at frequencies from 1 to 200 Hz with steps of 1 Hz.

It was found that there is a difference in velocity depending on what storey you are situated at, when looking at the vertical vibration spread. The transmission through the apartment separating wall, diagonally in the house, did not show the same behavior. Moreover it does not seem to matter a lot at which storey the disturbance is acting, it gives the same results at the other storeys anyway. The results from the two weaker models do not differ much from each other, but the velocities in these are higher than in the stiffest

model.

A lot of simplifications were made in the model, perhaps other ways of doing it would show other results. It is however most important to show what possibilities a full scale model like this can give. A new range of analyses can be made that were not possible before.

Contents

Nomenclature

A	Cross-sectional area $[m^2]$
a	Width of a shell [m]
$\mathbf{B}$	Gradient of the shape function $\left[\frac{N}{m^2}\right]$
b	Length of a shell [m]
c_B	Speed of bending waves $\left[\frac{m}{s}\right]$
$\mathbf{C}$	Damping matrix $\left[\frac{Ns}{m}\right]$
$\mathbf{C}$	Compliance matrix $[Pa^{-1}]$
γ	Shear strain
$\mathbf{D}$	Constitutive matrix [Pa]
δ	Normal displacement [m]
δ	Logarithmic decrement
E	Young's modulus [Pa]
ε	Normal strain
F	Force [N]
f	Frequency [Hz]
$\mathbf{f}$	External force vector [N]
$\mathbf{f}_b$	Boundary vector [N]
$\mathbf{f}_l$	Load vector [N]
$\mathbf{\Phi}$	Mode shapes
G	Shear modulus [Pa]
h	Height [m]
I	Second moment of inertia $[m^4]$
k_b	Bending stiffness parameter $\left[\frac{N}{m^2}\right]$
k_t	Normal stiffness parameter $\left[\frac{N}{m}\right]$
$\mathbf{K}$	Stiffness matrix $\left[\frac{N}{m}\right]$
κ	Curvature
L	Length [m]
L_{dB}	Vibrational level [dB]
λ	Wavelength [m]
λ_r	Eigenvalue $\left[\frac{1}{s^2}\right]$
M	Moment per unit length [N]

m	Mass [kg]
$\mathbf{M}$	Mass matrix [kg]
N	Force per unit length $\left[\frac{N}{m}\right]$
$\mathbf{N}$	Shape function
$\mathbf{n}$	Unit vector
ν	Poisson's ratio
q	Surface force $\left[\frac{N}{m^2}\right]$
θ	Ring angle [°]
ρ	Area density $\left[\frac{kg}{m^2}\right]$
σ	Stress [Pa]
t	Time [s]
$\mathbf{T}$	Transformation matrix
u	Displacement in the x-direction [m]
$\mathbf{u}$	Displacement vector [m]
$\dot{\mathbf{u}}$	Velocity vector $\left[\frac{m}{s}\right]$
$\ddot{\mathbf{u}}$	Acceleration vector $\left[\frac{m}{s^2}\right]$
V	Shear force per unit length $\left[\frac{N}{m}\right]$
v	Displacement in the y-direction [m]
w	Displacement in the z-direction [m]
$\ddot{w}$	Acceleration in the z-direction $\left[\frac{m}{s^2}\right]$
ω	Angular frequency [Hz]
ξ	Damping ratio

Chapter 1

Introduction

1.1 Background

Wood is one of our oldest construction materials but on the other hand also one of our newest. Since the end of the 19th century it has been prohibited in Sweden to construct wood-framed buildings with more than two storeys for reasons of fire safety. In 1994 a change of the *Swedish Construction Code* of *Boverket*, *BKR 94*, allowed to build more than two storeys made of wood. The construction code is now based on function and not material. At the same time research at different fields concerning building in wood started. In Sweden the resources of wood are big and now there is a growing interest of constructing multi-storey buildings and infrastructure in wood. In Northern America the tradition of constructing higher wood buildings is longer and widespread.

It has been shown that using wood as construction material gives rise to lower CO_2-emissions than other materials. In a particular study [6] a comparison of the energy consumption and the CO_2-emission was done for the whole life cycle (100 years) of a wood building and a fictive building instead made of concrete. The results show that the net emission of CO_2 is lower for wood buildings.

Today, when building houses, no dynamic simulations are made. The buildings are designed to meet the demands of stability and resistance. However there are two other problem areas that have to be taken into account when building with wooden frames: sound and vibration. The vibration of a wall or floor will cause pressure variations of the air, i.e. sound. The vibration itself can also be disturbing. It can stimulate other items in the room to oscillate

and the floor may be too flexible when people are moving in the building. Which vibrations that are experienced as disturbing varies from person to person, but in general people are most sensitive for $4-8$ Hz vibrations. The reason is that the inner organs easily vibrate at these frequencies, [3]. New techniques and further knowledge of vibration transmission in higher buildings are an important concern.

At the moment the highest buildings in Sweden made of wood are the seven-storey buildings of *Limnologen* situated in Växjö, which will be completed in the autumn of 2008. *Limnologen* is a part of the new urban district *Välle Broar*, where wood will be the common used construction material.

1.2 Objective and method

Improvements regarding sound and vibration transmission are of interest when constructing multi-storey wood buildings. The long term goal of research in these areas is to find a good way of building houses where residents are not disturbed by the noise and motion from the neighboring apartments. This thesis is a part of a project at Växjö University examining step sounds and vibrations at *Limnologen*.

The aim of the master thesis is to investigate how vibrations are spread through a wood building. This will be done by developing a FE-model for the seven-storey buildings at *Limnologen*. On this big scale FE-model new types of analyses are performed to answer questions like: Are there any differences between the storeys' dynamic behaviors depending on where they are situated? Does it matter where the excitation force is acting?

Only structure-borne sound is taken into account. No fluid-structure interaction is considered, i.e. air is not included in the model. Moreover only the energy-rich flexural waves are investigated.

1.3 Disposition

The report includes the following chapters:

- In Chapter 2 the phenomenons of air- and structure-borne sound are described and the instruments that are used to measure these quantities are presented.
- In Chapter 3 the material wood and its properties are treated.

- In Chapter 4 the theories of shells, the finite element method, modal analysis, damping and harmonic excitation are summarized.
- In Chapter 5 the quarter *Limnologen*, its building parts and the construction materials are presented.
- In Chapter 6 the implementation of the floor structure, the ceiling and the apartment separating wall in *Abaqus* is described.
- In Chapter 7 the transformation of a complicated continuum part to a simple shell part is derived.
- In Chapter 8 the implementation of the whole building with shell elements and the different load cases are presented.
- In Chapter 9 the results from the analyses are summarized.
- In Chapter 10 the results are discussed and conclusions are drawn.
- The last chapter contains suggestions for further work.

Chapter 2

Vibrations in buildings

2.1 Air- and structure-borne sound

In order to provide comfortable living conditions for residents in wood buildings one has to deal with the problems of air- and structure-borne sound. Sound is vibrational energy that propagates in terms of waves. Its source can for example be voices, steps or loudspeakers, which create pressure variations in the air. When this pressure variation reaches the ear the eardrum starts to vibrate and we pick it up as sound. For humans, hearing is limited to frequencies between about 20 and 20 000 Hz. When the pressure variation reaches a building part like a wall, the structure starts to vibrate, which then causes a new sound wave with reduced intensity on the other side of the wall.

Air-borne sound travels through air, hence its name. For structure-borne sound the transmission path from source to receiver takes place in a solid body like a wall or a floor. In the example of the wall above the sound changes from air-borne to structure-borne and back to air-borne.

Sound can propagate as longitudinal or transverse waves. The first wave type means particle motion in the same direction as the wave propagation and in transverse waves the particles move perpendicular to the direction in which the wave is travelling. Transverse waves do not exist in air. In thin structures as beams and plates sound can also propagate as bending waves, also called flexural waves.

Direct sound transmission is the propagation of sound through the wall or floor in a room, as indicated by number 1 in figure 2.1. Flanking transmission occurs when sound is travelling from one room to another indirectly,

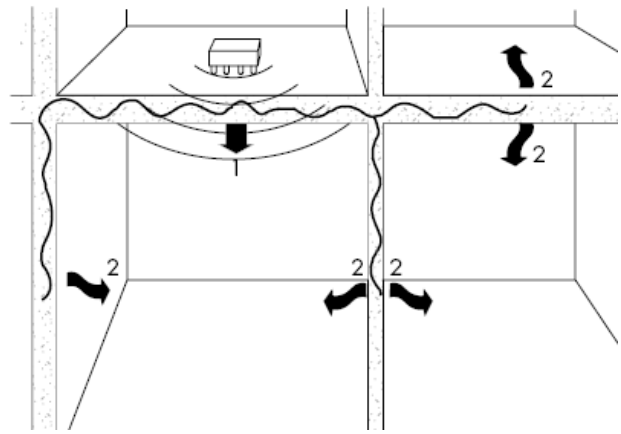

Figure 2.1: Direct and flanking transmission

through parts of the building other than the wall or floor. This is indicated by number 2 in figure 2.1. Other examples of flanking transmission pathways are windows, light switches, ventilation paths and waste pipes.

In this thesis only structure-borne sound is analyzed. It is supposed to be caused by an impact like from a vibrating machine or foot steps. The transition from structure-borne to air-borne sound is neglected. This implies that an air gap in between a wall does not transmit any sound, which is not true in reality. Moreover only bending waves are studied, since they are rich of energy and therefore most important for sound radiation. [2]

2.2 Measurements

In order to measure how structure-borne sound is propagating through a building two instruments are needed: A tapping machine and accelerometers.

A tapping machine is an impact sound generator used for standardized impact sound measurements. It consists of five hammers each weighing 0.5 kg that drop from a standard height of 40 mm twice a second, giving an operating frequency of 10 Hz. The vibration from the tapping machine is transmitted through the building. Figure 2.2 shows a photo of a tapping machine of the Danish manufacturer *Brüel and Kjaer*.

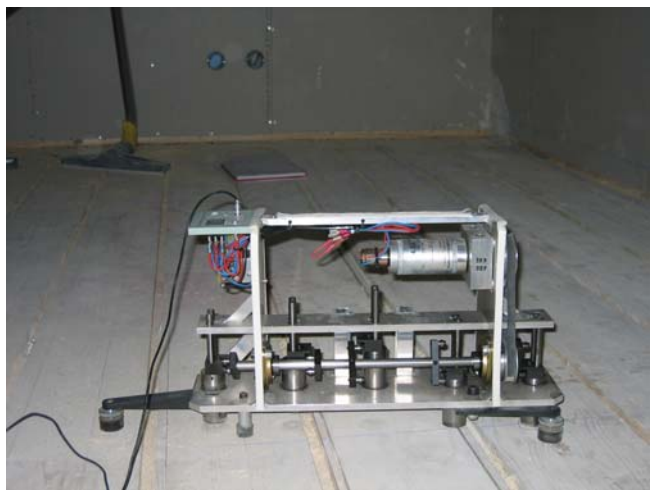

Figure 2.2: Tapping machine without casing

Vibrations can be measured as displacement, velocity or acceleration. An accelerometer is an electromechanical device that measures acceleration forces in three directions. As shown in figure 2.3 accelerometers are screwed on the building parts, where they measure the accelerations they are exposed to.

Figure 2.4 shows a possible measuring set-up: The accelerometers are attached to the floor structures, ceilings and walls of four rooms. In room 1 the tapping machine is producing standardized impacts and the response is measured in that room as well as in the three neighboring rooms.

The output of a system can also be expressed as *vibrational level* which expresses the ratio between the velocity of a signal and a reference velocity v_{ref}:

$$L_{dB} = 10log_{10}\left|\frac{v}{v_{ref}}\right|, \tag{2.1}$$

where $v_{ref} = 5 \cdot 10^{-8} m/s$. The unit of the vibrational level is *dB*.

Usually a signal is passed through a *Butterworth filter* to remove unwanted signal components and a response that is as flat as possible in the passband is created. For more information about the Butterworth filter see [17].

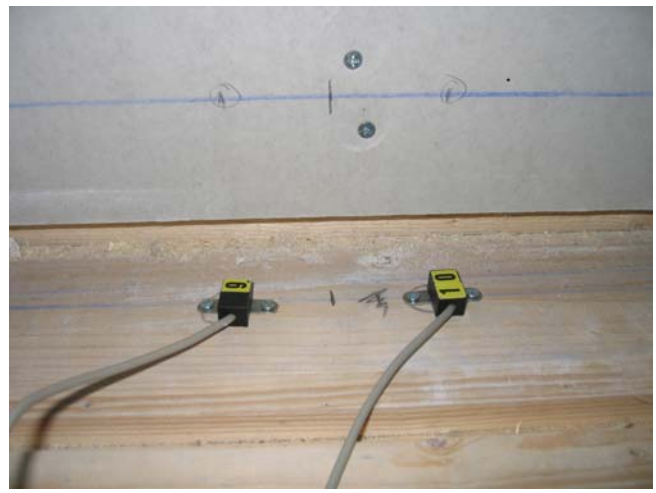

Figure 2.3: Accelerometers

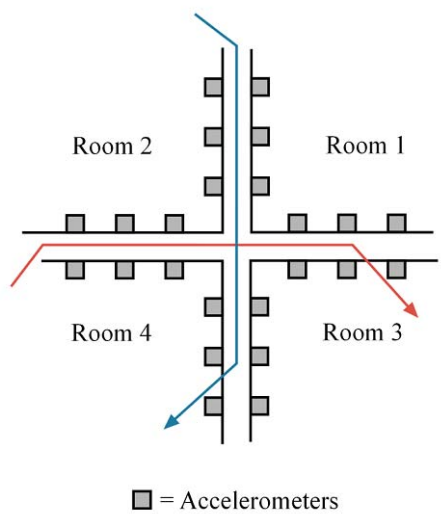

Figure 2.4: Measuring set-up

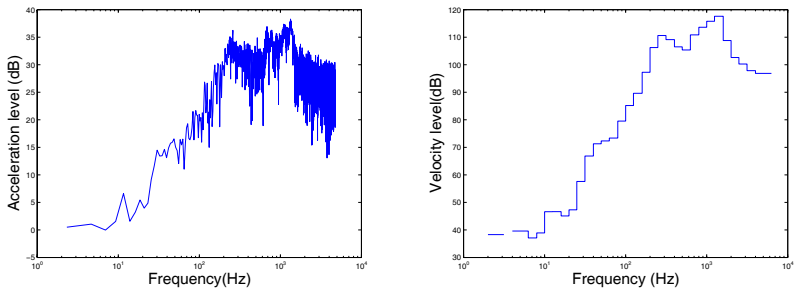

Figure 2.5: Example of measuring results

Figure 2.5 a shows an example of vibrational level (accelerations) calculated from some of the measured accelerations. The second figure shows the vibrational level of a signal when it has passed a Butterworth filter and is plotted as stairs.

In acoustics an interpolation of the accelerations over all measuring points (preferably the whole floor or wall) is done to get a mean value for the floor. By doing so differences within the floor are not recognized or taken into account and the properties are smeared out on the whole structure.

Chapter 3

Wood

3.1 General properties

Wood is a natural, cellular material which mainly consists of cellulose, hemicellulose and lignin. The cellulose and hemicellulose form fibrils and the lignin is cementing the fibrils together providing fibers. This makes it an heterogenous and anisotropic material. Wood is also hygroscopic, it adapts its moisture content after the environment either by absorption or adsorption.

There is a whole range of variables influencing the mechanical and physical properties of wood. Environmental modifiers are: moisture content, temperature and biological deterioration. Other factors affecting the properties are density, chemical content, whether the wood is grown in spring (*earlywood*) or fall (*latewood*) or its position in the trunk etc. The mechanical properties may vary a great deal within the same timber. Every single piece is unique and there are not two identical pieces of wood, as shown in figure 3.1.

The fact that wood is composed of fibers makes it an anisotropic material. Anisotropy means that the mechanical properties are not the same in different directions. How the material behaves depends on the direction it is loaded in. It is impossible to take full account of all heterogeneities, since every single knot and discontinuity of every piece of the lumber would have to be investigated. In this study, when modelling wood, it is considered as a homogenous orthotropic material, there are three perpendicular symmetry planes. One direction is parallel to the fibers (longitudinal), the other two are perpendicular in the radial and tangential direction. The fibers are aligned with the geometric coordinate system, as shown in figure 3.2. This is a simplification since the RLT-system is much likely to not coincide with

Figure 3.1: The radial and tangential direction can vary within a piece of sawn wood.

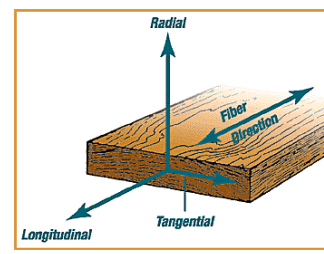

Figure 3.2: The figure illustrates the principal directions in a piece of wood.

the geometric system, xyz. In reality the L-axis can differ from the y-axis by an angle called *grain angle* and the T-axis from the z-axis by an angle called *ring angle*.

3.2 Constitutive modelling of wood

In order to describe an orthotropic material nine independent constants are needed. Three Young's moduli (E_x, E_y and E_z), three shear moduli (G_{xy}, G_{yz} and G_{xz}) and at last three independent poisson's ratios (ν_{xy}, ν_{yz} and ν_{xz}). The compliance matrix, $\mathbf{C}$, explains the relation between the strains and the

stresses and Hooke's law, $\boldsymbol{\varepsilon} = \mathbf{C}\boldsymbol{\sigma}$, is valid:

$$\begin{pmatrix} \varepsilon_{xx} \\ \varepsilon_{yy} \\ \varepsilon_{zz} \\ \gamma_{yz} \\ \gamma_{zx} \\ \gamma_{xy} \end{pmatrix} = \begin{pmatrix} \frac{1}{E_x} & -\frac{\nu_{yx}}{E_y} & -\frac{\nu_{zx}}{E_z} & 0 & 0 & 0 \\ -\frac{\nu_{xy}}{E_x} & \frac{1}{E_y} & -\frac{\nu_{zy}}{E_z} & 1 & 0 & 0 \\ -\frac{\nu_{xz}}{E_x} & -\frac{\nu_{yz}}{E_y} & \frac{1}{E_z} & 0 & 1 & 0 \\ 0 & 0 & 0 & \frac{1}{G_{yz}} & 0 & 1 \\ 1 & 0 & 0 & 0 & \frac{1}{G_{zx}} & 0 \\ 0 & 1 & 0 & 0 & 0 & \frac{1}{G_{xy}} \end{pmatrix} \begin{pmatrix} \sigma_{xx} \\ \sigma_{yy} \\ \sigma_{zz} \\ \sigma_{yz} \\ \sigma_{zx} \\ \sigma_{xy} \end{pmatrix}. \tag{3.1}$$

In the above compliance matrix three of the six poisson's ratios are not independent, they are related to the other three by:

$$\frac{\nu_{yx}}{E_y} = \frac{\nu_{xy}}{E_x} \tag{3.2}$$

$$\frac{\nu_{xz}}{E_x} = \frac{\nu_{zx}}{E_z} \tag{3.3}$$

$$\frac{\nu_{zy}}{E_z} = \frac{\nu_{yz}}{E_y}. \tag{3.4}$$

This gives a symmetric compliance matrix, $C_{ij} = C_{ji}$.

The following properties are valid for Norway spruce:

E_L	E_T	E_R	G_{LR}	G_{RT}	G_{TL}	ν_{RL}	ν_{TR}	ν_{LT}
$12000MPa$	$500MPa$	$800MPa$	$700MPa$	$34MPa$	$700MPa$	0.02	0.31	0.51

Table 3.1: Material properties of Norway spruce

The mechanical properties in the tangential and radial direction do not differ a lot. Therefore in construction codes the same properties are assigned to the radial and tangential directions. Hence modelling lumber as a transversely isotropic material is a natural approach. In the case of transverse isotropy there exists one plane where the mechanical properties are isotropic. For that case Hooke's law is given by:

$$\begin{pmatrix} \varepsilon_{xx} \\ \varepsilon_{yy} \\ \varepsilon_{zz} \\ \gamma_{yz} \\ \gamma_{zx} \\ \gamma_{xy} \end{pmatrix} = \begin{pmatrix} \frac{1}{E_p} & -\frac{\nu_{tp}}{E_t} & -\frac{\nu_p}{E_p} & 0 & 0 & 0 \\ -\frac{\nu_{pt}}{E_p} & \frac{1}{E_t} & -\frac{\nu_{pt}}{E_p} & 0 & 0 & 0 \\ -\frac{\nu_p}{E_p} & -\frac{\nu_{tp}}{E_t} & \frac{1}{E_p} & 0 & 0 & 0 \\ 0 & 0 & 0 & \frac{1}{G_p} & 0 & 1 \\ 0 & 0 & 0 & 0 & \frac{1}{G_t} & 0 \\ 0 & 0 & 0 & 0 & 0 & \frac{1}{G_p} \end{pmatrix} \begin{pmatrix} \sigma_{xx} \\ \sigma_{yy} \\ \sigma_{zz} \\ \sigma_{yz} \\ \sigma_{zx} \\ \sigma_{xy} \end{pmatrix}, \tag{3.5}$$

where p denotes in-plane properties (here in the RT(XZ)-plane) and t perpendicular to the plane (L(Y)-direction). In the isotropic plane the following relation is valid:

$$G_p = \frac{E_p}{2(1+v_p)}. \tag{3.6}$$

In total five independent material constants are needed to describe the transversely isotropic material. The following section shows how to obtain representative values of the in-plane properties, E_p and G_p, from the values in table 3.1.

3.3 Material orientations

In structural applications there is generally no knowledge of how the ring and grain angles are oriented in the lumber. Representative values of Young's and shear modulus are needed in order to consider the possible orientations of the ring angle. A ring angle differing from zero leads to lumber where loads are applied that are not aligned with one of the symmetry axes and the moduli have to be transformed in order to formulate the relation between stresses and strains. The grain angle can also vary within the sawn wood, the wood is cross-grained. That means that the fibers are not aligned with the geometric coordinate system. It is more likely that the grain angle is closer to zero than the ring angle. An assumption is that the grain angle is zero in the lumber, i.e. the L-axis coincides with the y-axis.

To obtain Hooke's law in the geometric coordinate system the stresses $\boldsymbol{\sigma}$ and strains $\boldsymbol{\varepsilon}$ in the plane are transformed to the geometric coordinate system according to:

$$\overline{\boldsymbol{\sigma}} = \mathbf{T}\boldsymbol{\sigma} \tag{3.7}$$

$$\overline{\boldsymbol{\varepsilon}} = \mathbf{T}\boldsymbol{\varepsilon}, \tag{3.8}$$

where $\mathbf{T}$ is the transformation matrix:

$$\mathbf{T} = \begin{pmatrix} \cos^2\theta & \sin^2\theta & 2\sin\theta\cos\theta \\ \sin^2\theta & \cos^2\theta & -2\sin\theta\cos\theta \\ -\sin\theta\cos\theta & \sin\theta\cos\theta & \cos^2\theta - \sin^2\theta \end{pmatrix}. \tag{3.9}$$

Equations 3.7 and 3.8 together with Hooke's law, $\boldsymbol{\varepsilon} = \boldsymbol{C}\boldsymbol{\sigma}$, give:

$$\overline{\mathbf{C}} = \mathbf{T}\mathbf{C}\mathbf{T}^{-1}, \tag{3.10}$$

which is the law of transformation for the orthotropic compliance parameters.

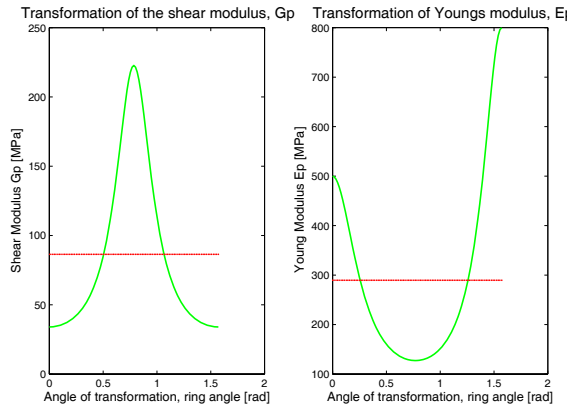

Figure 3.3: The figure illustrates the transformation of E_p and G_p with regard to the ring angle.

The elements of the transformed compliance matrix $\overline{\mathbf{C}}$ are:

$$\overline{C_{11}} = C_{11}\cos^4\theta + (2C_{12} + C_{66})\sin^2\theta\cos^2\theta + C_{22}\sin^4\theta \tag{3.11}$$

$$\overline{C_{22}} = C_{11}\sin^4\theta + (2C_{12} + C_{66})\sin^2\theta\cos^2\theta + C_{22}\cos^4\theta \tag{3.12}$$

$$\overline{C_{66}} = 4\left(C_{11} + C_{22} - 2C_{12}\right)\sin^2\theta\cos^2\theta + C_{66}\left(\cos^2\theta - \sin^2\theta\right)^2, \tag{3.13}$$

where $C_{11} = \frac{1}{E_R}$, $C_{22} = \frac{1}{E_T}$, $C_{12} = \frac{\nu_{TR}}{E_T}$ and $C_{66} = \frac{1}{G_{RT}}$.

The ring angle is varied between 0° and 90° and the matrix elements $\overline{C_{11}}$, $\overline{C_{22}}$ and $\overline{C_{66}}$ are computed for each possible angle. Then E_p and G_p are calculated: $E_p = \frac{1}{\overline{C_{11}}}$ and $G_p = \frac{1}{\overline{C_{66}}}$. An average over these is taken, as shown in figure 3.3. For further information on wood and its properties see [1], [5] and [14].

Chapter 4

Theory

4.1 Shell theory

A shell is a structure whose thickness h is small compared to all other dimensions. Shells can be curved and they carry both membrane and bending forces.

The theory of shells is an approximation which reduces the three-dimensional problem to a simpler two-dimensional problem. Plane stress is assumed. The shell is loaded by a distributed surface-force q in the negative z-direction. For the definition of the coordinate system see figure 4.1. The xy-plane is located in the mid-plane of the shell, and u resp. v are the displacements of the mid-plane in the x- and y-directions, respectively. The deflection w is measured as positive in the z-direction.

The bending moments per unit length (M_{xx} and M_{yy}) and the twisting moments per unit length (M_{xy} and M_{yx}) are calculated from the stress components that exist for sections normal to the x- and y-axes [16]:

$$M_{xx} = \int_{-h/2}^{h/2} z\sigma_{xx} dz \tag{4.1}$$

$$M_{yy} = \int_{-h/2}^{h/2} z\sigma_{yy} dz \tag{4.2}$$

$$M_{xy} = M_{yx} = \int_{-h/2}^{h/2} z\sigma_{xy} dz. \tag{4.3}$$

The normal forces per unit length in the x- and y-direction (N_{xx} and N_{yy}) and the horizontal shear forces per unit length (N_{xy} and N_{yx}) are calculated

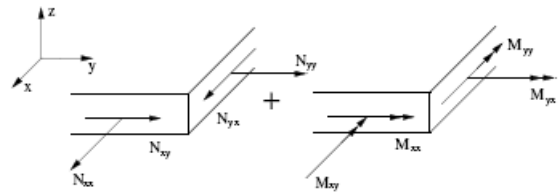

Figure 4.1: Moments and forces acting on the shell [16]

in a similar way:

$$N_{xx} = \int_{-h/2}^{h/2} \sigma_{xx} dz \tag{4.4}$$

$$N_{yy} = \int_{-h/2}^{h/2} \sigma_{yy} dz \tag{4.5}$$

$$N_{xy} = N_{yx} = \int_{-h/2}^{h/2} \sigma_{xy} dz. \tag{4.6}$$

The moments and forces acting on the shell are shown in figure 4.1.

Hooke's law is given by

$$\boldsymbol{\sigma} = \boldsymbol{D}\boldsymbol{\varepsilon} - z\boldsymbol{D}\boldsymbol{\kappa}, \tag{4.7}$$

where the stresses $\boldsymbol{\sigma}$, strains $\boldsymbol{\varepsilon}$ and curvatures $\boldsymbol{\kappa}$ are expressed by the following vectors:

$$\boldsymbol{\sigma} = \begin{bmatrix} \sigma_{xx} \\ \sigma_{yy} \\ \sigma_{xy} \end{bmatrix} \tag{4.8}$$

$$\boldsymbol{\varepsilon} = \begin{bmatrix} \varepsilon_{xx} \\ \varepsilon_{yy} \\ \gamma_{xy} \end{bmatrix} = \begin{bmatrix} \frac{\partial u}{\partial x} \\ \frac{\partial v}{\partial y} \\ \frac{\partial u}{\partial y} + \frac{\partial v}{\partial x} \end{bmatrix} \tag{4.9}$$

$$\boldsymbol{\kappa} = \begin{bmatrix} \kappa_{xx} \\ \kappa_{yy} \\ \kappa_{xy} \end{bmatrix} = \begin{bmatrix} \frac{\partial^2 w}{\partial x^2} \\ \frac{\partial^2 w}{\partial y^2} \\ 2\frac{\partial^2 w}{\partial x \partial y} \end{bmatrix}. \tag{4.10}$$

The plane stress constitutive matrix for orthotropic elasticity is written

$$\boldsymbol{D} = \begin{pmatrix} D_{11} & D_{12} & 0 \\ D_{12} & D_{22} & 0 \\ 0 & 0 & D_{33} \end{pmatrix} = \begin{pmatrix} \frac{E_x}{1-\nu_{xy}\nu_{yx}} & \frac{\nu_{xy}E_y}{1-\nu_{xy}\nu_{yx}} & 0 \\ \frac{\nu_{yx}E_x}{1-\nu_{xy}\nu_{yx}} & \frac{E_y}{1-\nu_{xy}\nu_{yx}} & 0 \\ 0 & 0 & G_{xy} \end{pmatrix}. \tag{4.11}$$

The moments and forces can then be written as

$$\boldsymbol{M} = \begin{bmatrix} M_{xx} \\ M_{yy} \\ M_{xy} \end{bmatrix} = \int_{-h/2}^{h/2} \boldsymbol{\sigma} z dz = \boldsymbol{D\varepsilon} \int_{-h/2}^{h/2} z dz - \boldsymbol{D\kappa} \int_{-h/2}^{h/2} z^2 dz = -\frac{h^3}{12} \boldsymbol{D\kappa} \tag{4.12}$$

$$\boldsymbol{N} = \begin{bmatrix} N_{xx} \\ N_{yy} \\ N_{xy} \end{bmatrix} = \int_{-h/2}^{h/2} \boldsymbol{\sigma} dz = \boldsymbol{D\varepsilon} \int_{-h/2}^{h/2} dz - \boldsymbol{D\kappa} \int_{-h/2}^{h/2} z dz = \boldsymbol{D\varepsilon} h. \tag{4.13}$$

Hence the stiffness relation of a shell section may be expressed as:

$$\begin{pmatrix} N_{xx} \\ N_{yy} \\ N_{xy} \\ M_{xx} \\ M_{yy} \\ M_{xy} \end{pmatrix} = \begin{pmatrix} hD_{11} & hD_{12} & 0 & 0 & 0 & 0 \\ hD_{12} & hD_{22} & 0 & 0 & 0 & 0 \\ 0 & 0 & hD_{33} & 0 & 0 & 0 \\ 0 & 0 & 0 & -\frac{h^3}{12}D_{11} & -\frac{h^3}{12}D_{12} & 0 \\ 0 & 0 & 0 & -\frac{h^3}{12}D_{12} & -\frac{h^3}{12}D_{22} & 0 \\ 0 & 0 & 0 & 0 & 0 & -\frac{h^3}{12}D_{33} \end{pmatrix} \begin{pmatrix} \varepsilon_{xx} \\ \varepsilon_{yy} \\ \gamma_{xy} \\ \kappa_{xx} \\ \kappa_{yy} \\ \kappa_{xy} \end{pmatrix}. \tag{4.14}$$

This relation is valid for a structure with a reference plane that is coinciding with a plane trough the center of mass (neutral plane) and for which the shear center coincides with the torsional center. That means that a normal force applied on the shell will not create any curvature κ_{xx} resp. κ_{yy} and a moment will not cause any normal strain ε_{xx} resp. ε_{yy} on the neutral plane. Secondly a shear state will not generate any shear curvature κ_{xy} and a torsion no shear strain γ_{xy}. All this means that the bending and normal behavior are uncoupled.

Love's equations for an orthogonal shell that is loaded by a distributed surface force q are [18]:

$$-\frac{\partial V_{xz}}{\partial x} - \frac{\partial V_{yz}}{\partial y} + \rho h \ddot{w} = q, \tag{4.15}$$

where

$$V_{yz} = \frac{\partial M_{xy}}{\partial x} + \frac{\partial M_{yy}}{\partial y} \tag{4.16}$$

and

$$V_{xz} = \frac{\partial M_{xx}}{\partial x} + \frac{\partial M_{xy}}{\partial y}. \tag{4.17}$$

Substituting equation 4.16 and 4.17 into equation 4.15 gives:

$$\frac{\partial^2 M_{xx}}{\partial x^2} + 2\frac{\partial^2 M_{xy}}{\partial x \partial y} + \frac{\partial^2 M_{yy}}{\partial y^2} + q = \rho h \ddot{w}. \tag{4.18}$$

Substitution of equation 4.12 into equation 4.18 gives:

$$\frac{h^3}{12}\left(D_{11}\frac{\partial^4 w}{\partial x^4} + 2\left(D_{12}+2D_{33}\right)\frac{\partial^4 w}{\partial x^2 \partial y^2} + D_{22}\frac{\partial^4 w}{\partial y^4}\right) + \rho h \ddot{w} = q. \tag{4.19}$$

This is the shell equation for an orthotropic shell.

4.1.1 Speed of the propagating waves

There is a range of different waves propagating in an elastic medium. The speeds of the different wave types are not the same. For longitudinal and transverse waves they are a material property, i.e. they are only dependent of the elastic properties and the density of the material in question. For orthotropic materials, as wood, the speed will be dependent on the direction of propagation. For flexural waves in shells the wave speed also depends on the frequency and the cross-sectional thickness [15]:

$$c_B(\theta) = \sqrt{\omega}\sqrt[4]{\frac{D(\theta)}{\rho h}}, \tag{4.20}$$

where ω is the angular frequency of the wave, ρ is the density of the shell, h is its height and θ is the angle between the direction of propagation and the x-axis. The stiffness $D(\theta)$ is:

$$D(\theta) = \frac{h^3}{12}\left(\frac{E_x \cos^4(\theta)}{1-\nu_{xy}\nu_{yx}} + 2\left(\frac{\nu_{xy}E_y}{1-\nu_{xy}\nu_{yx}} + 2G\right)\cos^2(\theta)\sin^2(\theta) + \frac{E_y \sin^4(\theta)}{1-\nu_{xy}\nu_{yx}}\right) \tag{4.21}$$

The relation between the wavelength, frequency and velocity of a wave is given by:

$$\lambda = \frac{c_B}{f}. \tag{4.22}$$

4.2 The finite element method

The finite element method is a numerical approach used to find approximate solutions of partial differential equations. It is applicable to a huge number of physical problems. The domain to be analyzed is divided into small elements of finite size (*finite elements*). Each element has specific material properties and boundary conditions, which are known at certain points of the elements, the so called *nodal points*. The way in which the variable changes between

these points can be linear, quadratic, cubic, etc. Calculations are carried out on each element and the behavior of every element is obtained. In the end all elements are assembled to achieve the behavior of the whole structure. The assemblage of all elements is called *mesh*. It is important to chose a realistic mesh size. A too fine mesh will cause unnecessary computational cost, but a too coarse mesh will not give a good approximation of the solution.

The standard dynamic FE-formulation is

$$\mathbf{M\ddot{u}} + \mathbf{C\dot{u}} + \mathbf{Ku} = \mathbf{f}. \tag{4.23}$$

$\mathbf{K}$ is the global stiffness matrix. It includes the geometry and the material properties of the structure. $\mathbf{u}$ is the displacement vector, which contains the displacements of the nodal points of the structure. $\dot{\mathbf{u}}$ is the velocity vector, $\ddot{\mathbf{u}}$ the acceleration vector, $\mathbf{M}$ is the mass matrix and $\mathbf{C}$ is the damping matrix. $\mathbf{f}$ contains the external forces applied at the nodal points of the structure. It can be divided into two vectors:

$$\mathbf{f} = \mathbf{f}_b + \mathbf{f}_l, \tag{4.24}$$

where $\mathbf{f}_b$ is the boundary vector and $\mathbf{f}_l$ is the load vector.

4.2.1 FE-formulation of shells

For shell elements the global stiffness matrix, the boundary vector and the load vector are defined in the following way:

$$\mathbf{K} = \frac{h^3}{12}\int_A \mathbf{B}^T\mathbf{D}\mathbf{B}dA \tag{4.25}$$

$$\mathbf{f}_b = \oint_L \mathbf{N^T}\left(V_{nz} + \frac{dM_{nm}}{dm}\right)dL - \oint_L (\nabla\mathbf{N})^T\,\mathbf{n}M_{nn}dL \tag{4.26}$$

$$\mathbf{f}_l = \int_A \mathbf{N}^T q dA. \tag{4.27}$$

$\mathbf{N}$ contains the shape functions and $\mathbf{B}$ the gradient of $\mathbf{N}$:

$$\mathbf{B} = \begin{pmatrix} \frac{\partial^2\mathbf{N}}{\partial x^2} \\ \frac{\partial^2\mathbf{N}}{\partial y^2} \\ 2\frac{\partial^2\mathbf{N}}{\partial x\partial y} \end{pmatrix}. \tag{4.28}$$

V_{nz} is the vertical shear force per unit length acting on the section defined by the unit vector $\mathbf{n}$, M_{nn} is the bending moment per unit length and M_{nm} is the twisting moment per unit length. $\left(V_{nz} + \frac{dM_{nm}}{dm}\right)$ is the effective shear force per unit length. [16]

4.3 Modal analysis

Modal analysis is the method of finding the natural frequencies and mode shapes of a structure. When a structure is exposed to a disturbance it vibrates at its *natural frequencies*. Structures have an unlimited number of natural frequencies. An FE-model has as many modes as there are degrees of freedom. They depend on the structure's mass and stiffness. If the frequency of the perturbation force is close to one of the structure's natural frequencies the amplitude and acceleration of the vibration will become very high. This is called *resonance* and it is a phenomenon that should be avoided in all structures. For each of the natural frequencies the dynamic response is different. The different deformation shapes are called *modes* or *mode shapes*. The mode belonging to the lowest natural frequency is the *fundamental mode*. Integer multiples of the fundamental frequency are the *harmonics*, while the remaining multiples are called *overtones*.

For the determination of the natural frequencies and their modes the unloaded structure is analyzed and damping is neglected. The equation of motion 4.23 is then

$$\mathbf{M\ddot{u}} + \mathbf{Ku} = \mathbf{0} \tag{4.29}$$

with the solutions

$$\mathbf{u} = A\cos wt\mathbf{\Phi}. \tag{4.30}$$

Substitution of equation 4.30 into equation 4.29 gives

$$\mathbf{K\Phi} = \omega^2\mathbf{M\Phi}, \tag{4.31}$$

which can be written as

$$(\mathbf{K} - \lambda\mathbf{M})\mathbf{\Phi} = \mathbf{0}. \tag{4.32}$$

This is an eigenvalue problem with N eigenvalues $\lambda_r (r = 1, 2, ..., N)$. $\mathbf{\Phi}_r$ are the corresponding eigenvectors or mode shapes. The natural frequencies of the structure are $\omega_r = \sqrt{\lambda_r}$.

The eigenvalue problem has a nontrivial solution if

$$det(\mathbf{K} - \lambda\mathbf{M}) = 0. \tag{4.33}$$

For more information about modal analysis see [4].

4.4 Damping

In a dynamical analysis of a structure damping is always present in various ways, internally in the material, as friction in joints, contact zones etc. It

is possible to apply the damping as material damping, which is a material property, that in wood also depends on the direction. Material damping originates from non-linearities in the material, i.e. discontinuities. The logarithmic decrement, δ, is given for spruce: $\delta = 0.02$ in the fiber direction and $\delta = 0.024$ perpendicular to the fibers [12]. In an experiment described in [10] full scale experiments of two-storey timber frames were carried out and it was suggested to apply additional damping in the range of 1-5 %. A damping of 3 % was used in this project. The relation between the logarithmic decrement and the damping ratio is:

$$\xi = \frac{\delta}{\sqrt{4\pi^2 + \delta^2}}. \tag{4.34}$$

The mass participation is highest for the lowest modes with the lowest eigenfrequencies. That means that the response, which is composed of a combination of all the modes will contain more of the lower ones. Therefore it is most important to damp the lower frequencies. In structures also damping from joints etc. is modelled as material Rayleigh damping which is proportional to the mass and the stiffness matrix according to:

$$\mathbf{C} = \alpha\mathbf{M} + \beta\mathbf{K}, \tag{4.35}$$

where the damping ratio for mode n is given as:

$$\xi_n = \frac{\alpha}{2}\frac{1}{\omega_n} + \frac{\beta}{2}\omega_n. \tag{4.36}$$

As stated by the formula, α is mostly important for the lower modes and β is mostly important for the higher frequencies. This means that the lower frequencies are damped with the mass and the damping forces depend on the absolute velocities of the model. The higher frequencies are damped by the stiffness and the damping is proportional to the strain rate [17]. Since the stiffness of a non-linear system may increase during the analysis and the Rayleigh-coefficients are based on the initial stiffness, this can lead to convergence problems [10]. A natural approach is therefore to use only mass proportional damping leading to $\alpha = 2\omega_n\xi_n$. The damping ratio is different for all modes. An approximation is done when using the same α-value for all of them. More information about damping can be found in [4].

4.5 Harmonic excitation of damped systems

A system is under harmonic excitation when an external force F_0 of a single frequency ω is applied on it. The equation of motion of such a system is

given by [11]:

$$\mathbf{M\ddot{u}} + \mathbf{C\dot{u}} + \mathbf{Ku} = F_0 \cos(\omega t). \tag{4.37}$$

The forced response of the damped system has the same form with the same frequency as the driving force but with different amplitude and phase. The total response of the input is composed of both the homogeneous and the particular solution, $u(t) = u_h(t) + u_p(t)$.

$$u(t) = \underbrace{e^{-\xi\omega_n t}(A\cos\omega_d t + B\sin\omega_d t)}_{u_h(t)} + \underbrace{C\sin\omega t + D\cos\omega t}_{u_p(t)}, \tag{4.38}$$

where ω_n is the eigenfrequency and $\omega_d = \omega_n\sqrt{1-\xi^2}$ is the damped frequency. A, B, C and D depend on the initial values. It is seen that the homogeneous solution approaches zero for large values of t and high damping ξ, i.e. it is transient. The particular solution is the remaining part, i.e. the steady-state response. It is common that the transient part is ignored and only the steady-state response is considered.

Chapter 5

Limnologen

The four buildings at *Limnologen* in Växjö are the highest buildings in Sweden constructed with a load-bearing framework made of wood. The ground floor is casted in concrete, but the rest of the bearing framework (seven floors) is entirely made of wood. Every floor is divided into five apartments with varying size. The side of the building that is facing northeast is having a glue-laminated timber facade (figure 5.1) and the opposite side is covered with plaster (figure 5.2). Just the topmost story's facade is made all the way of glue-laminated timber.

Martinsons byggsystem AB is the manufacturer of the prefabricated building parts, e.g. floor structures and walls used within the apartment. The wood species is *Norway Spruce* which is the spruce growing in Scandinavia.

The floor structure stretch between the exterior walls on the two long sides of the building. In apartments that are continuous between these two sides the floor structures are supported about midways by a bearing wall or a beam. To solve noise problems the ceiling is not in contact with the floor structure and just hung up between the walls. The individual apartments are separated by an air gap, but at several points there are fixations connecting the floor structures of two neighboring apartments to transfer the horizontal forces in the building.

5.1 Building parts

For the transmission of vibrations through the house four building parts are important: The floor structure, the ceiling, the apartment separating wall and the inner wall.

Figure 5.1: Facade facing southwest

Figure 5.2: Facade facing northeast

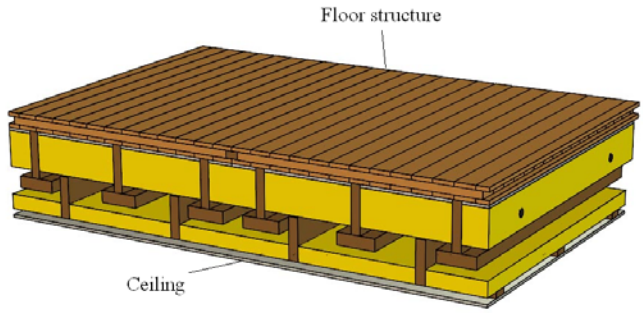

Figure 5.3: This is the floor element, floor structure and ceiling, made by *Martinsons Byggsystem AB.* [13]

5.1.1 Floor structure

The floor structure is the upper part of the floor element, as shown in figure 5.3. The top is made out of three layers of massive timber. The middle layer is rotated 90 degrees with respect to the two outer layers. Underneath these layers some wooden T-beams are positioned. They are made of glue-laminated timber and are stiffening the floor structure in its longitudinal direction. Between the beams there is an insulation layer. The floor structures are manufactured with a width of 1.2 meters and in various lengths.

5.1.2 Apartment separating wall

In order to reduce the sound transmission between different apartments a special kind of wall is used. The construction of the apartment separating wall is formed to reach the demands of sound insulation, which are classified with ”sound class” A, B or C, in this case sound class B. An important purpose of the apartment separating wall is to prevent fire from easily spreading between the apartments.

The apartment separating wall is a part of the vertical bearing frame composed by studs with a center distance of 600 mm. A board is connected to the studs on top of which battens are fastened with a center distance of 450 mm. The outer parts are two gypsum boards, *Protect F 15*, which are screwed onto the battens. Between the beams, both studs and battens, there is a wood fiber insulation. The wall is composed of two layers like this sepa-

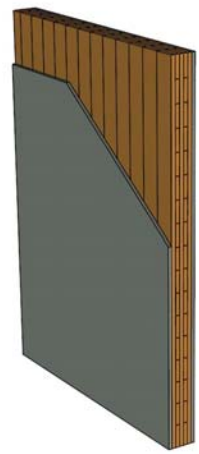

Figure 5.4: This is an example of an inner wall containing five layers of massive wood and one gypsum board. [13]

rated by a 20 mm air gap. This air gap prevents mechanical vibrations from passing directly between the walls.

5.1.3 Ceiling

The ceiling is the lower part of the floor element, shown in figure 5.3. It is made of massive wood studs and battens which are orthogonal to each other. Two 13 mm gypsum boards are fastened on the battens. The studs and battens are making the structure stiffer in both directions. Between the studs some wood fiber insulation is placed.

5.1.4 Inner wall

The rooms in each apartment are separated by massive wood walls. Some are composed of three layers and some of five layers. Every layer is rotated 90 degrees with respect to its neighboring layers, as shown in figure 5.4. Some inner walls contain a gypsum layer on each side.

5.2 Material

5.2.1 Massive wood

The massive timber in the floor structure is made of *Norway Spruce*. The moisture content in construction timber for indoor use is about 12 %. The density of the wood is assumed as 440 kg/m^3 [14]. The five independent parameters describing *Norway spruce* as transversely isotropic are:

E_L	$E_R = E_T$	$G_{LR} = G_{LT}$	G_{RT}	ν_{RL}
$12000MPa$	$300MPa$	$700MPa$	$90MPa$	0.02

Table 5.1: Material properties of Norway spruce

5.2.2 Glue-laminated timber

Parts of the floor structure as well as some vertical columns and horizontal beams are made of glue-laminated timber. Pieces of timber are glued together in several layers making up stronger and longer beams. This is a common construction element, since it has a high strength-to-mass ratio and is available in a whole range of lengths. Beams as long as 60 meters can be produced.

The properties of glue-laminated timber, class *L40*, are [19]:

E_L	$E_R = E_T$	$G_{LR} = G_{LT}$	G_{RT}	ν_{RL}
$13000MPa$	$450MPa$	$850MPa$	$90MPa$	0.02

Table 5.2: Material properties of glue-laminated timber

5.2.3 Plasterboard

Gypsum is used because of its fire resistant properties. The gypsum board contains calcium sulfate bonded in hydrates. The water is vaporized when exposed to the heat of fire. As long as there is water left in the gypsum board, it will delay the heat transfer. Gypsum is modelled as an isotropic material with the following properties, [8]:

E	ν	ρ
$2250MPa$	0.3	$847kg/m^2$

Table 5.3: Material properties of plasterboard

5.2.4 Board

Hard wood fiber board is an example of an engineered wood product commonly used on construction sites all over the world. It is industrially manufactured and, as the name indicates, it consists of wood fibers. With high steam pressure the wood fibers are separated and ground into a mass mixed with liquid. The wet mass is then pressed to form the boards. The fiber board is modelled as homogeneous and isotropic. The properties of *K-40* board are [19]:

E	G	ρ
$5000MPa$	$2100MPa$	$900kg/m^2$

Table 5.4: Material properties of board

Chapter 6

FE-model of the building parts

6.1 Finite element software

Abaqus is a software for finite element analyses developed by SIMULIA. It is divided into three products: *Abaqus/Standard*, *Abaqus/Explicit* and *Abaqus/CAE*.

Abaqus/Standard is a general implicit solver for static, dynamic and thermal finite element problems, including nonlinear problems. A global stiffness matrix is created and a system of equations is solved implicitly at the end of each solution increment. This solution method is unconditionally stable and the solution is not affected by the time increment.

Abaqus/CAE provides a complete modelling and visualization environment, where it is possible to create finite element models to carry out analyses and to evaluate data. Usually the model is created in *Abaqus/CAE*, then the numerical problem is solved in *Abaqus/Standard* or *Abaqus/Explicit* and in the end postprocessing is done in *Abaqus/CAE*.

6.2 Implementation of the building parts into *Abaqus*

All parts were modelled with $C3D8R$-elements of size 0.05 m. This is a continuum element with three degrees of freedom at each node, translations in all directions. There are eight nodes in the element, one at each corner which are interpolated linearly. R means that it uses reduced integration. A high order of numerical integration gives less additional approximation into

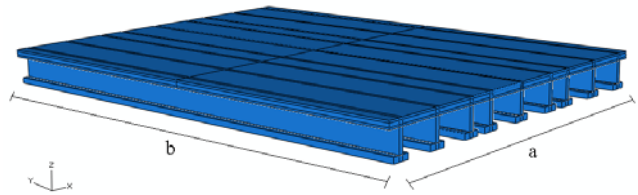

Figure 6.1: FE-model of the floor structure

the FE-method and full integration gives a better result. A problem of using full integration is though that the stiffness is overestimated and shear-locking may occur. Because of that fact, reduced integration leads to a more accurate FE-solution. On the other hand, first order (linear) elements and reduced integration may cause spurious zero-energy modes. A zero-energy mode is a mode where no elastic energy is created, which is true only for rigid-body motions. In this case an element with one integration point may distort in a way that leads to zero strain in the integration point even though it is not a rigid-body motion. Hourglass control is adopted to avoid this phenomena,[16] [17].

No nails or screws were included in the simulations. Neither were any contact zones modelled. Instead the constraint `tie` represented the connections, which means that there are no relative motions between the surfaces of two instances. Moreover the insulation layers were not included in the model, since they do not transfer any vibrations. The modes for each of the building parts were calculated and the different mode shapes were analyzed. For this analysis the building parts were fixed at all four sides.

6.2.1 Floor structure

A FE-model of the floor structure is shown in figure 6.1. As a reference the width $a = 3.6$ m and the length $b = 4.8$ m were chosen. The model consisted of 45 162 elements with 212 868 degrees of freedom.

It was noticed that, for a large number of modes, the beams were displaced in the horizontal direction only, shown in figure 6.2. These modes are not of interest for further analyses, because they are not excited when loaded by a vertical force as from a footstep or a tapping machine. The important modes are the ones where the massive wood layers are displaced vertically, as in figure 6.3.

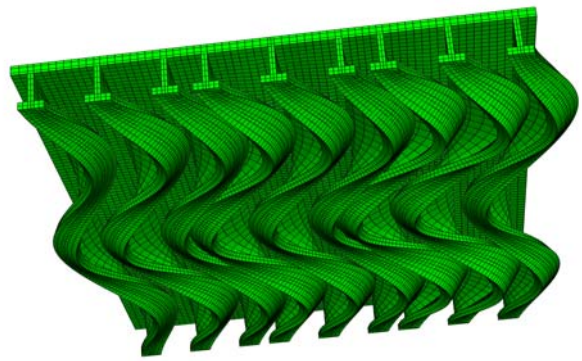

Figure 6.2: Mode 45 - Only the beams are bent.

The motion of the beams is also absorbing energy. As the mass is not distributed in an even way because of the beams there are further modes not as good-looking as in figure 6.3. There are a lot of modes where only a part of the floor structure is active (see figure 6.4) making them hard to identify.

6.2.2 Apartment separating wall

As a reference model, representing the apartment separating wall, a part with the dimensions 3.65 m x 2.922 m was modelled. $b = 2.922$ m is the height of all apartment separating walls and $a = 3.65$ m was chosen so that the boundaries contain both battens and studs, see figure 6.5. The model contained 19 240 elements with 121 950 degrees of freedom.

In the model the two gypsum boards were represented as a homogeneous part with twice the thickness of a single one. This fact may neglect some additional damping that occurs from the contact between the boards. Moreover the stiffness of having two boards on top of each other will become lower than one with twice the thickness. The friction in the contact zone absorbs energy which is neglected when modelling as one. The consequence is that the damping is underestimated which needs to be compensated for with a global damping of the building. The complex geometry of the wall made it

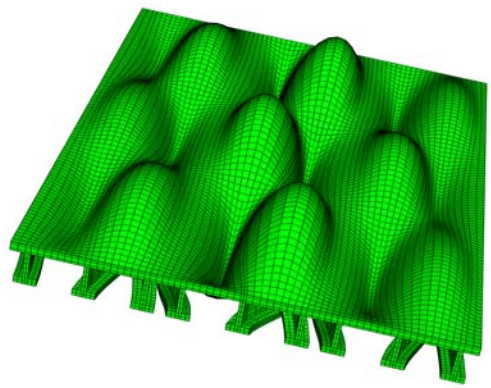

Figure 6.3: Mode 35 - Displacement of the massive wood layers.

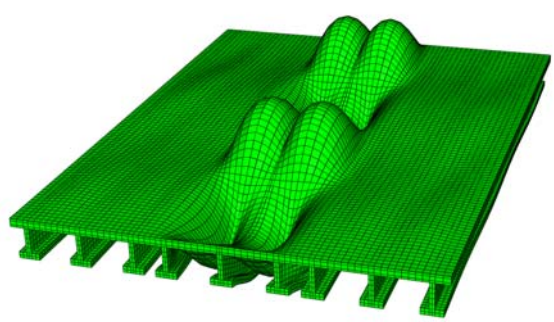

Figure 6.4: Mode 65 - Only some parts of the massive wood layers are active.

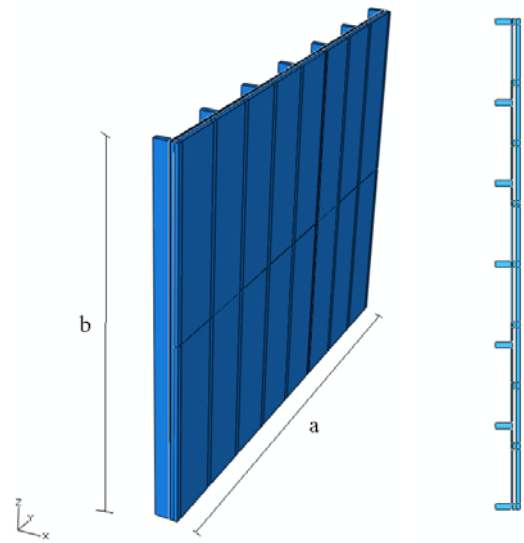

Figure 6.5: The reference model of the apartment separating wall (side view and top view)

difficult to find a global behavior for the whole structure. Due to the various distances of the battens and the studs the vibrational patterns of the gypsum boards and the board differed.

An investigation of the modes and natural frequencies showed that the gypsum and the board are primarily moving, while the stiffer studs remain stiller. The weak properties of the gypsum board and the loose connection makes them vibrate easily. In that way energy is absorbed and thus prevented from being transmitted to the bearing frame where it can be transmitted further through the building.

As already mentioned, the dynamic properties of a structure, as the apartment separating wall, are complex. It was observed that a motion of the board also leads to a torsion of the studs, see figure 6.6.

6.2.3 Ceiling

The FE-model of the ceiling is shown in figure 6.7. It has a width of $a = 3.6$ m and a length of $b = 4.27$ m. The total number of elements was 15 034 with 98 952 degrees of freedom. Also the ceiling has modes where only the battens

Figure 6.6: Examples of how the studs in the walls are twisted

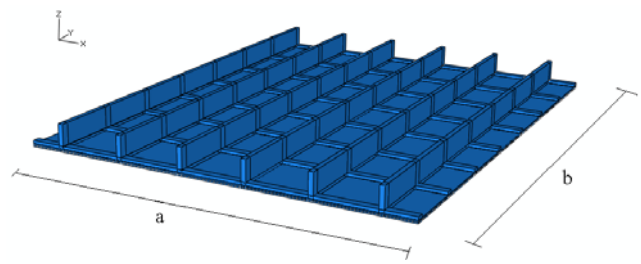

Figure 6.7: FE-model of the ceiling

are displaced. Again these modes are not of interest for the calculations.

Chapter 7

Equivalent properties

The building is a very complex structure that results in a FE-model with an enormous number of degrees of freedom. This would require too much disk space and computational cost. Therefore the building parts had to be simplified. Instead of continuum elements shell elements were used for floor structure, ceiling and apartment separating walls.

7.1 Strategy for finding equivalent stiffness properties

Each shell should in its dynamic behavior correspond as good as possible to the reference building part. To achieve this the stiffness and mass of the corresponding structures must be the same. To define the stiffness of a shell four parameters are needed: E_x, E_y, G_{xy} and ν_{xy}. Three analyses were made on each reference building part (in *Abaqus*) to obtain these material parameters. The analyses carry out loading in bending, tension and torsion, where the respective displacements and torsion angles are calculated. From these the stiffness was computed. By replacing the reference structure with a shell the global stiffness for static analyses are satisfied, but some dynamic properties may be lost due to the complexity of the structures.

The height of each shell was chosen as $h = 0.15$ m and the length and width were the same as in the corresponding reference model, i.e. $a_{new} = a$ and $b_{new} = b$.

A problem that appeared when calculating Young's modulus was that different values were obtained from the bending and normal loading. Different ideas of solving this were discussed. An approach was to divide the shell into

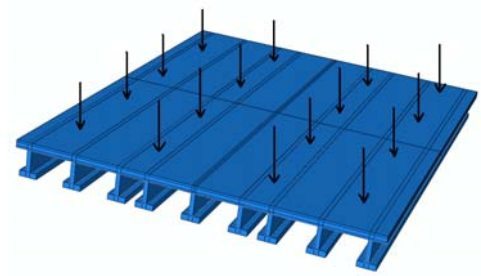

Figure 7.1: The bending analysis

several layers with different fictive material properties. This led to negative Young's moduli for some layers. Since the theory and software do not approve negative material parameters, even though the composite globally has a positive stiffness, this idea was rejected. One way of avoiding this problem is to directly specify the section stiffness of each shell in the model. This is done by a matrix that relates curvatures to moments and strains to forces and that depends on both material and shape, according to equation 4.14. In order to mind that Young's moduli for bending resp. normal loading are not the same, different Young's moduli were used in the lower resp. upper half of the matrix. The following three sections show how the stiffness parameters in the stiffness matrix were computed.

7.1.1 Young's modulus by a bending and tension analysis

Young's modulus by a bending analysis

The reference building part was fixed at two opposite sides. It was loaded with a distributed surface force of $1000N/m^2$ in the negative z-direction, which was applied on the whole upper side of the building part, as shown in figure 7.1.

For a beam which is fixed at both ends and loaded with a distributed line load q the relation

$$q = k_b \cdot w \tag{7.1}$$

holds [9], where w is the displacement of the center of mass in the z-direction and

$$k_b = \frac{384 E_b I}{L^4} \tag{7.2}$$

is the stiffness parameter. I is the beam's second moment of inertia, E_b is Young's modulus for bending and L is the beam's length.

To compare the reference building part with such a beam its surface force was expressed as a distributed line force

$$q = 1000\frac{N}{m^2} \cdot (\text{length of the part's fixed side}). \tag{7.3}$$

This line force and the obtained displacement w of the building part were substituted into equation 7.1 to calculate the stiffness parameter.

Two bending analyses were made, one with the reference building part's longer sides fixed (i.e. $L = a_{new}$) to obtain a value for the stiffness in the x-direction, and one with its shorter sides fixed (i.e. $L = b_{new}$) to obtain the stiffness in the y-direction.

The second moments of inertia for the two cases of bending are

$$I_x = \frac{b_{new}h^3}{12} \tag{7.4}$$

$$I_y = \frac{a_{new}h^3}{12}. \tag{7.5}$$

Substitution of the second moments of inertia into equation 7.2 gives Young's modulus in the x- and y-direction:

$$E_{bx} = \frac{k_{bx}a_{new}^4}{32b_{new}h^3} \tag{7.6}$$

$$E_{by} = \frac{k_{by}b_{new}^4}{32a_{new}h^3}. \tag{7.7}$$

Young's modulus by a tension analysis

The normal stiffness of the shell section was determined by fixing the reference building part at one side. A distributed tension force $1000N/m^2$ was acting on the other side, as shown in figure 7.2. The displacement at the side where the tension force was acting was measured.

The normal stiffness k_t of a bar is the relation between the force F and the displacement δ [9]:

$$F = k_t\delta, \tag{7.8}$$

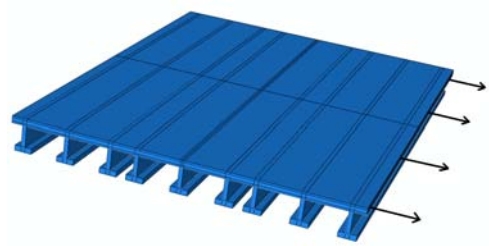

Figure 7.2: The first tension analysis

where the normal stiffness is:

$$k_t = \frac{E_t A}{L}. \tag{7.9}$$

A is the cross-sectional area and L is the length of the bar.

In order to compare the reference building part with a bar its distributed force was expressed as a point force

$$F = 1000\frac{N}{m^2} \cdot (\text{area of the part's torn side}). \tag{7.10}$$

Again two analyses were made on the reference building part: tension in the x- and y-direction.

Substitution of the areas $A_x = b_{new}h$, $A_y = a_{new}h$ and lengths $L_x = a_{new}$, $L_y = b_{new}$ into equation 7.9 gives Young's modulus in the x- and y-direction:

$$E_{tx} = \frac{a_{new}k_{xt}}{b_{new}h} \tag{7.11}$$

$$E_{ty} = \frac{b_{new}k_{yt}}{a_{new}h}. \tag{7.12}$$

7.1.2 Shear modulus by a torsion analysis

To determine the shear modulus of the shell, the reference building part was fork supported at one of the shorter sides, i.e. displacement in the x- and z-direction and torsion around the y-axis were restrained. As translation in the y-direction was not restrained, it was possible for the building part to warp and Saint-Venants torsion theory [7] was applied for calculations. At

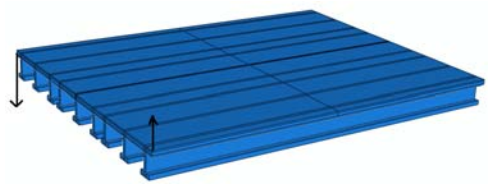

Figure 7.3: The torsion analysis

the opposite side the reference building part was loaded with a twisting moment of $M_{xy} = 3600Nm$ around the y-axis and the rotation θ due to this moment was measured. The loading situation is shown in figure 7.3.

The reference building part was then replaced by a shell which rotated by the same angle θ when loaded with the moment M_{xy}.

Because of the torsion around the y-axis the xy-plane of the shell is shifted in the x-direction. The different points on a line perpendicular to the plane are shifted differently depending on their distance to the center line, i.e. $z = 0$. The shear strain is

$$\gamma_{xy} = \frac{z \cdot \theta}{b_{new}}. \tag{7.13}$$

The relation between the shear stress and the shear strain is

$$\sigma_{xy} = G_{xy}\gamma_{xy}. \tag{7.14}$$

The shear stress can be related to the moment as [16]:

$$M_{xy} = \int_{-\frac{h}{2}}^{\frac{h}{2}} z\sigma_{xy}dz \cdot a_{new}. \tag{7.15}$$

Substitution of equation 7.14 and 7.13 into equation 7.15 and computation of the integral gives

$$G_{xy} = \frac{12M_{xy}b_{new}}{a_{new}\theta h^3}. \tag{7.16}$$

7.1.3 Poisson's ratio by a tension analysis

To extract the global poisson's ratio of the structure another tension analysis was performed. Distributed surface forces acting on two opposite sides of the building part were applied, as shown in figure 7.4. In order to let the

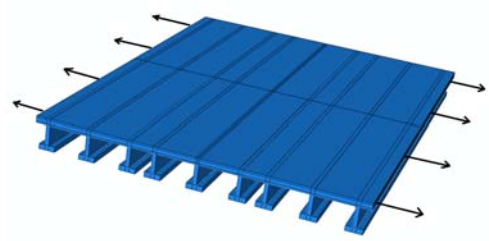

Figure 7.4: The second tension analysis

reference building part contract in the plane no side was fixed. Instead it was possible for the part to deform in all directions. Since the strains are compared in order to calculate the poisson's ratio rigid body motions will not affect the result. One degree of freedom needs to be fixed though in order to avoid a singular stiffness matrix during the FE-calculation.

Poisson's ratio ν_{xy} describes the relation between the strains in two different directions. When a force is acting in the x-direction, the normal strain ε_{xx} is present. There are also normal strains in the other directions. The strain in the y-direction ε_{yy} is related to ε_{xx} according to:

$$\nu_{xy} = -\frac{\varepsilon_{yy}}{\varepsilon_{xx}}. \tag{7.17}$$

7.2 Density of the shell

The shell must also have the same mass m as the reference building part. The area of the shell is

$$A_{new} = a_{new} \cdot b_{new}, \tag{7.18}$$

which gives a area density of

$$\rho_{new} = \frac{m}{A_{new}} = \frac{m}{a_{new} b_{new}}. \tag{7.19}$$

7.3 Results

The following table sums up the material parameters of the shells that replaced the different building parts:

The analyses that were made on the reference building parts, as described

parameter	*floor structure*	*ceiling*	*apartment separating wall*
$\rho_{new}\,[kg/m^2]$	53.4	30.1	38.5
$E_{bx}\,[MPa]$	31.0	70.8	4.47
$E_{by}\,[MPa]$	26500	2080	12900
$E_{tx}\,[MPa]$	2550	518	481
$E_{ty}\,[MPa]$	7570	742	1670
$G_{xy}\,[MPa]$	353	23.8	64.8
ν_{xy} resp. ν_{yx}	$\nu_{xy} = 0.004045$	$\nu_{yx} = 0.2355$	$\nu_{yx} = 1.46 \cdot 10^{-4}$

Table 7.1: Material parameters of the shells replacing the building parts

in section 7.1, were also made on the shells to validate that the stiffness was implemented correctly. Some analyses were also conducted on reference parts and shells of varying sizes to confirm that the method is valid for dimensions that differ from the standard ones.

7.4 Choice of measuring points and consequences

When representing all these structures as shells some simplifications were made. As described in section 4.1 the uncoupled stiffness matrix is valid for cases where the neutral planes coincides with the reference plane. Complicated structures as the floor structure do not have a unique neutral plane because of the differing cross-sectional properties in the x- and y-direction. In theory there are two different neutral planes (no global neutral plane), one in each direction, and the stiffness matrix is therefore coupled.

The aim of the analyses was to capture a behavior considered to well represent the global behavior of the whole building part. For a simple shell made up of one material the global behavior is easy to obtain. The deflections are the same over the whole shell. In our cases the structures are more complicated, since they consist of beams, layers and other elements which are displaced differently, see figure 7.5. For that reason weighted averages over the building parts were taken, as described below.

7.4.1 Floor structure

As stated previously the beams only act as stiffeners in one direction. The global behavior can easily be represented by the top layers in the weak direc-

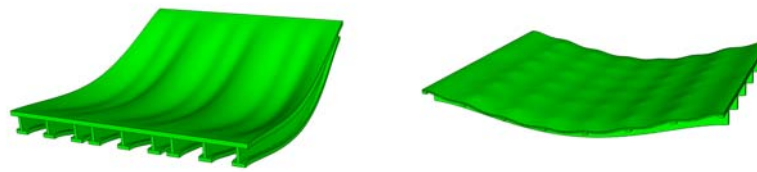

Figure 7.5: Deflection of floor structure and ceiling in the bending analysis

tion, since the beams have a small influence in this direction. In the stiffer direction bending led to one displacement for the beams and another for the top layers that are weaker, see figure 7.5 a. The values of the beams were chosen as the global behavior. For the tension analyses an average over the floor structure's height was chosen, when calculating the displacements, see figure 7.6.

When the modes/frequencies of the floor structure were compared with the modes of the equivalent shell, a quite good accordance was found for the lower modes. However, for higher frequencies, the dynamic properties of the floor structure and its equivalent shell differ increasingly with increasing frequency. The modes with only local deformations, as the one in figure 6.4, are not present in the shell structure.

To improve the results an approach of distributing the mass on the shell was made by resembling the mass distribution of the reference building part, i.e the approach of nonstructural mass was applied. However no significant improvement of the results was found. The fact that it is necessary to have an accurate knowledge of the positions of beams, studs and battens in the entire building in order to apply nonstructural mass led to the decision to neglect the more complicated mass distribution.

7.4.2 Apartment separating wall

The complex geometry of the apartment separating wall (board, gypsum, battens and studs) makes it impossible to capture its dynamic properties in

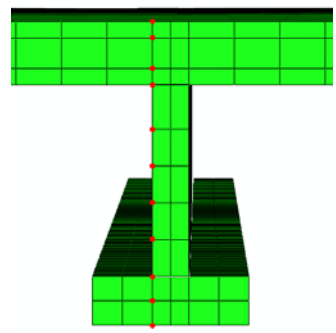

Figure 7.6: This figure shows the nodes over whose displacements an average is taken for the case of tension in the y-direction.

a shell. The decision was made to choose the behavior of the studs to account for the global behavior. The studs are a part of the bearing structure of the building and therefore flanking transmission from different apartments will act through the studs. By making this choice, the energy absorbing motions of the board and gypsum were not included in the model. When investigating the modes of the apartment separating wall, the studs were often twisted which is not possible to represent by using a shell structure. Because of that the agreement between the natural frequencies of the apartment separating wall and its corresponding shell was not very good.

7.4.3 Ceiling

The same type of bending behavior as in the stiffer direction of the floor structure and apartment separating wall was discovered in the ceiling structure, as shown in figure 7.5 b. The gypsum boards are weaker than the studs and therefore the global behavior was chosen to be based on the studs.

7.5 Suggestions for improvement of the model

For the ceiling and the wall there is no good consent between the modes/frequencies of the reference building part and the equivalent shell. The structures are too complex to represent their behavior with a simple shell only. The model may probably be improved significantly by taking into account that there

indeed is a coupling between bending and normal behavior.

An approach that is common, when modelling complicated structures, is to use substructures. These are collections of elements from which the internal degrees of freedom have been eliminated to reduce the size of the model. This can be very useful when the same substructure appears several times in a model, as the floor in a building. A lot of computational cost is saved by applying this approach compared to a model with all degrees of freedom remaining. The time frame of the master thesis did however restrict the possibilities of testing this method and to compare it with the technique of transforming a continuum body to a shell, as described in this chapter.

Chapter 8

FE-model of the building

A model of a representing part of the building was made up in *Abaqus*, including floor one to six. Figure 8.1 shows the region of the building that was chosen as the representing part. The region included three apartments, or parts of them, on each of the six identical storeys.

8.1 Geometry and mesh

Floor structure, ceiling and apartment separating walls were represented by shells with the material properties found in section 7.3. The inner walls were made up of laminated shells with three layers of massive wood. The exterior walls do not have the same properties as the apartment separating walls. However, in order to make a simple model, they were modelled as shells with the same material parameters as the apartment separating walls. All walls of an apartment were modelled as one part. Figure 8.2 shows the *Abaqus*-model of the building part.

In the real building, the floor structures are jointed together, since they are delivered in 1.2 meter wide pieces stretching from one long side of the building to the other. In the *Abaqus*-model however all the floor structures of one apartment were represented as one shell, which means that the interaction losses that may occur between the floor elements are not taken into account.

There are three columns in apartments 1 on each floor, which are made of glue-laminated timber and which are carrying part of the weight of the floor structure. These were modelled with connector elements of type $ProjCartesian$. This connector element has differing stiffness in the three translational direc-

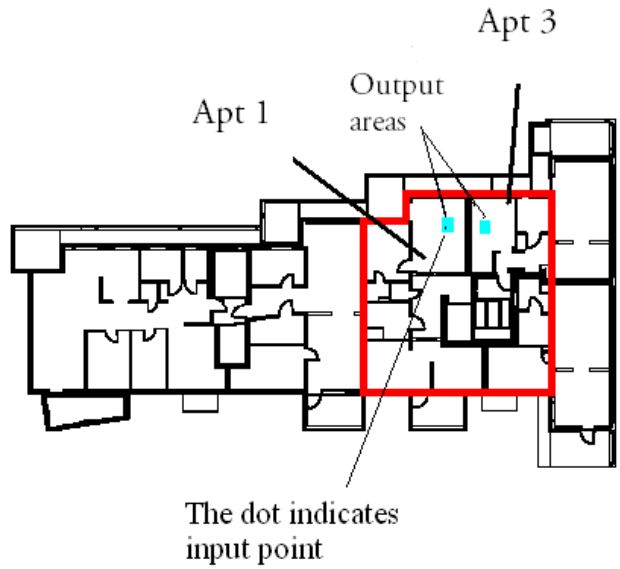

Figure 8.1: Modelled part of the building

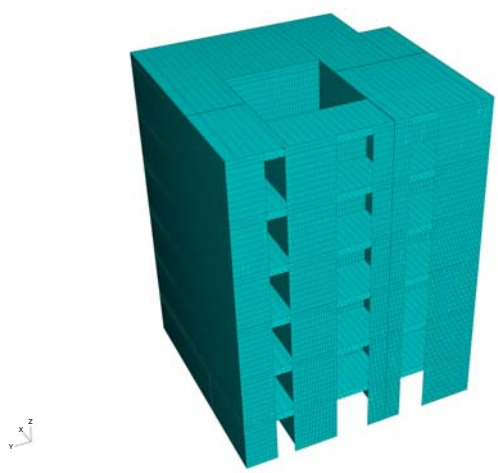

Figure 8.2: Model of a part of the building

tions:

$$k_x = \frac{3EI_x}{L^3} \tag{8.1}$$

$$k_y = \frac{3EI_y}{L^3} \tag{8.2}$$

$$k_z = \frac{AE}{L}, \tag{8.3}$$

where z is the direction of the long side of the column. E is Young's modulus of glue-laminated timber in the longitudinal direction, L is the length and A the cross-section area of the column. I_x and I_y are the second moments of inertia in the x- and y-direction, respectively.

Apartment 1 also contains two beams that lie on top of the columns. They are modelled as beam elements with the material properties of glue-laminated timber.

In a building, like the ones at *Limnologen*, there are a lot of details: fixations, lists, nails etc., the list is long. When creating a model of such a large structure small details like these need to be simplified or neglected. Modelling every nail and fixation in the model is very difficult and it might not be possible to know the exact number and position of all of them.

The properties of the different shells are varying. In order to use as few elements as possible in the model, a specific mesh was used for each part. As discussed in section 4.1.1 on page 20, the wavelength of the flexural waves is frequency dependent. In the stiffer direction the speed and wavelength is higher than in the weaker direction and therefore the mesh elements were chosen as being rectangular. There is an upper frequency limit for a given mesh, meaning that frequencies up to that value can be resolved. Since most of the energy is represented in the lower modes, a frequency of 500 Hz is chosen as limit of resolution. The size of the mesh was chosen according to this criteria. In the diagrams in figure 8.3 the speed and wavelength for different directions and parts are presented.

For a reasonable accuracy it is recommended that the shortest wavelength of interest should be represented by six internodal intervals [17]. This results in the element sizes in the x- and y-direction, shown in table 8.1:

The element type used through the analyses is $S4R$. This is a four-node conventional shell element that uses reduced integration. It has five degrees of freedom, three translations and two rotations. The element sizes in table 8.1

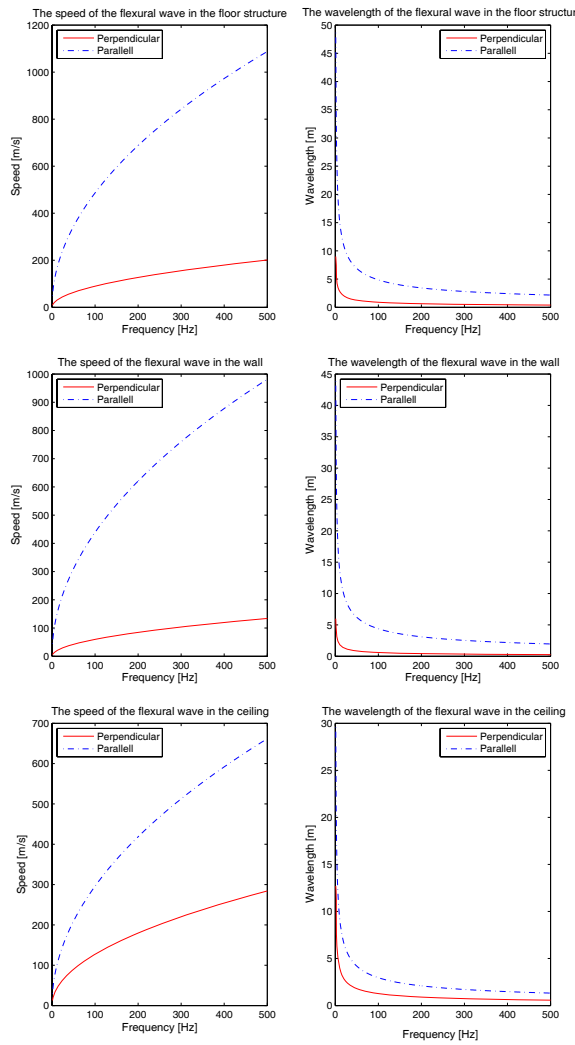

Figure 8.3: Speed and wavelength of the flexural waves in the different parts

	Floor structure	*Ceiling*	*Wall*
$x - dir$	$6.7cm$	$9.5cm$	$4.5cm$
$y - dir$	$36cm$	$22cm$	$32.7cm$

Table 8.1: Element sizes

lead to 211 557 elements with 2 752 110 degrees of freedom for the model of the building.

8.2 Modelling of the junctions and boundary conditions

There is a huge number of junctions in the building. The apartment separating walls are meeting the floor structure and the ceiling. The complex interactions between the building parts were simplified by fixed connections, i.e. the building parts cannot translate or rotate relative to each other. They were modelled with the surface-based *tie*-constraints. This procedure constraints the boundary degrees of freedom of two regions together. One will act as master and the degrees of freedom at the slave region will be the same as for the master. For best accuracy the region with the coarsest mesh is assigned to be master, in this case the floor structure and the ceiling.

The apartment separating walls contain a 20 mm wide air gap. That means that two apartments are not in direct contact with each other, but, as described earlier, there is a number of fixations between the floor structures of the apartments. These were modelled with connector elements of the type *join*, i.e. the relative translations of the floor structures were constrained in these points.

The walls of the first floor are connected to the ground floor that is made of concrete. This was modelled with fixed boundary conditions, i.e. all translations and rotations were restrained at the bottom edges of the building.

As mentioned before, the floor structures were connected to the walls with *tie*-constraints. It is difficult to model the constraints at the connecting points. A reasonable guess can be that they are not fixed and they are weaker in bending. Three models were made: one where the floor structures were entirely fixed to the walls and two where the connections were weaker in bending. This was solved with a row of elements at the edges of each

floor structure where different section properties are assigned. When these elements were assigned the same material properties as the floor structure it will act as fixed. To achieve the two other models some changes were done in the shell general section matrix. The elements describing bending, D_{44} and D_{55}, were a half and a forth of the original values. D_{44} was changed for all sides of the floor structures that were fixed at the walls in the x-direction and D_{55} in the y-direction. These models are referred to as `fixed`, `weak50` and `weak25`, where 50 and 25 denote that the stiffness against bending is 50 % and 25 % of the original.

8.3 Load cases and output

In the analyses, first a static step was performed, where the stresses and strains due to gravity loading were calculated. Secondly a steady-state dynamic step was performed from 1 Hz to 200 Hz in steps of 1 Hz. A steady-state dynamic step calculates only the steady-state response of the harmonic excitation and ignores the transient. A harmonic load of 700 N, approximately the weight of a person, was applied on the floor of apartment 1 at three different storeys (2, 4 and 6) at the position showed in figure 8.1.

Analysis results were calculated for apartment 1 and 3 and on all six floors. The results were shown as frequency-response curves of the velocity amplitudes and of the vibrational level. The velocities that are accounted for in the plots always come from all nodes within an area of approximately one square meter of the floor. The mean value was taken over these velocities. The position of the output areas is shown in figure 8.1. This procedure was done for all three models, thus 36 different output data sets were obtained.

Modal analyses were also performed for the building to compare the frequencies of the stiff building with the ones of the two weaker connection cases.

8.3.1 Modes and natural frequencies

Since there are many degrees of freedom in the model, there exist many natural frequencies and they are moreover very close in value. The differences between the natural frequencies are sometimes as low as a hundredth of a Hz. The natural frequencies are changing slightly when the section properties of the bending stiffness of the connection between the floor structures and walls are varied. A weaker connection gave natural frequencies that are slightly

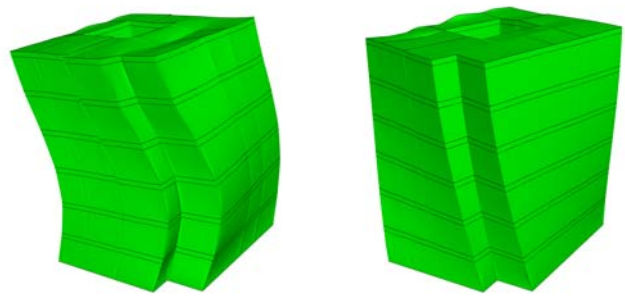

Figure 8.4: Modes related to motions of the whole building

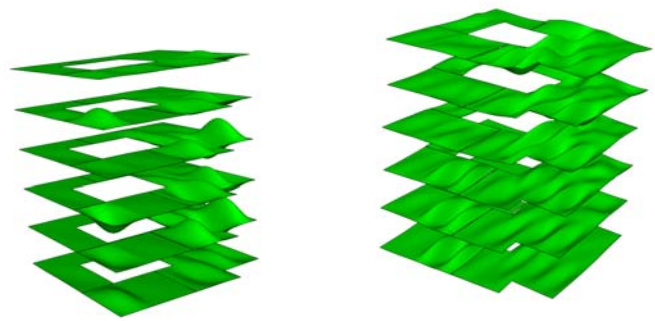

Figure 8.5: Examples of modes with natural frequencies of 38.6 Hz and 50.7 Hz

larger than for a stiffer connection. The lowest natural frequencies are of modes concerning motions of the whole building. Examples are shown in figure 8.4. It is highly unlikely that the modes in figure 8.4 are started with the excitation caused by a human step, however with the enormous forces of an earthquake they might occur. In the other modes the floor structures and walls are moving in all different kinds of combinations. Examples are shown in figure 8.5.

Chapter 9

Results of the vibrational simulations

The main task was to investigate how vibrations were transmitted in the wood-framed building. In order to do so some analyses were performed, as described in chapter 8. The excitation force was applied on the floor of apartment 1 on storey 2, 4 resp. 6 and the output was obtained at several storeys in apartment 1 as well as in apartment 3, as shown in figure 9.1. These three analyses were made for all three models; `fixed`, `weak50` and `weak25`. By combining the obtained vibrational data vertical, horizontal and diagonal transmission was analyzed. It was investigated how much of the vibrations was transmitted to different storeys in apartment 1 and how much was transmitted to the neighboring apartments (3). Different storeys were compared and it was analyzed if it makes a difference to replace the `fixed` model with models with more flexible joints (`weak50` and `weak25`). When comparing the output of the different models and load cases both velocities and vibrational levels were investigated. The vibrational level is calculated from the velocity as shown in equation 2.1. Figure 9.2 shows an example of the steady-state response with a harmonic excitation.

9.1 Comparison of the three models

This section treats a comparison of the results when different joints were used. Some interesting observations were made when analyzing the obtained velocity data. In general it can be stated that the plots of the `fixed`-model are having a different appearance than the ones of the two weaker models. For the `fixed`-model the peaks are wider and it usually has its highest peak at about 130 Hz. For both `weak50` and `weak25` the peaks are very narrow

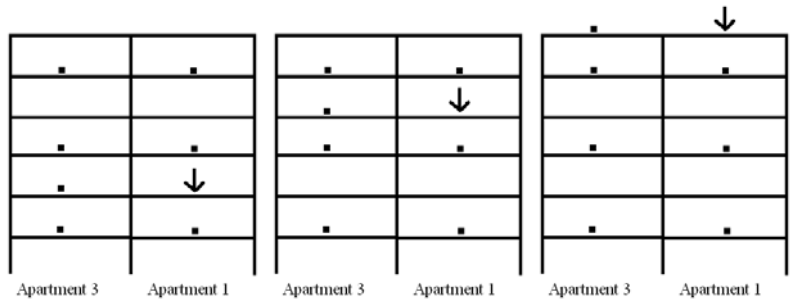

Figure 9.1: Excitation forces and output points

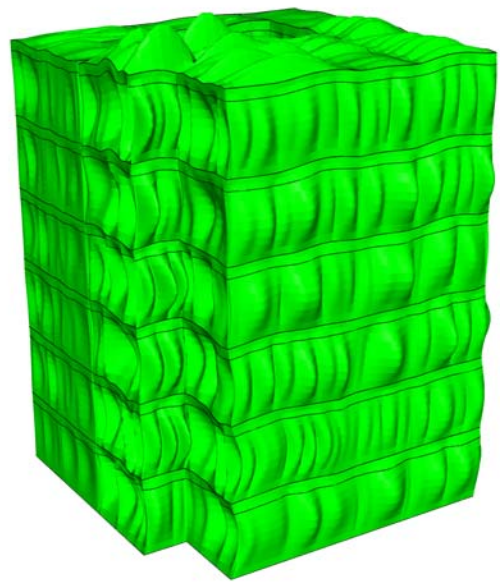

Figure 9.2: Steady-state response at 101 Hz

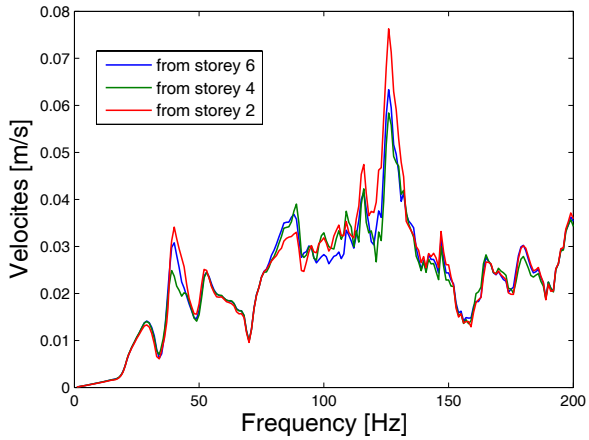

Figure 9.3: Velocities in apartment 1 storey 1 when excited at storey 6, 4 and 2 for model `fixed`

and reach larger values than `fixed`. The magnitude is about the same over all frequencies except for some outstanding peaks that always appear around 40 Hz. Figure 9.3 shows a typical plot for the `fixed`-model and figure 9.4 for the `weak25`-model. In this specific case the highest velocity for `weak25` is 0.33 m/s, while `fixed` not even reaches 0.08 m/s. Also the mean value for `weak25` is much larger than for `fixed`. For `weak25` the mean value is a bit higher than for `weak50`. In general it is observed that a change from `fixed` to a weaker model results in a much more drastic alteration of velocities and vibrational level than a change from `weak50` to `weak25`, see figure 9.5 and figure 9.6.

9.2 Comparison of the different storeys

The vibrations of the floors situated at different storeys were compared. Regarding apartment 1 it was found that the velocity was lower in the middle of the building as compared to under- and overlying storeys, as shown in figure 9.7. For frequencies below 40 Hz the top storey showed the largest velocity, while the velocity of the lowermost storey was largest when the frequency exceeded 40 Hz. This means that there in fact were differences in velocity level depending at which storey the output is obtained. These differences were less significant in the weaker models: The largest difference

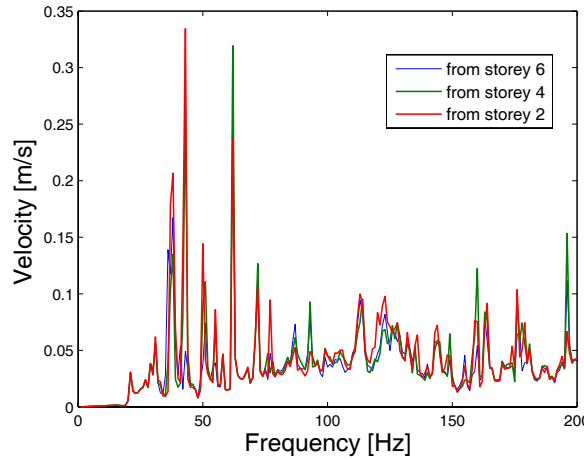

Figure 9.4: Velocities in apartment 1 storey 1 when excited at storey 6, 4 and 2 for model `weak25`

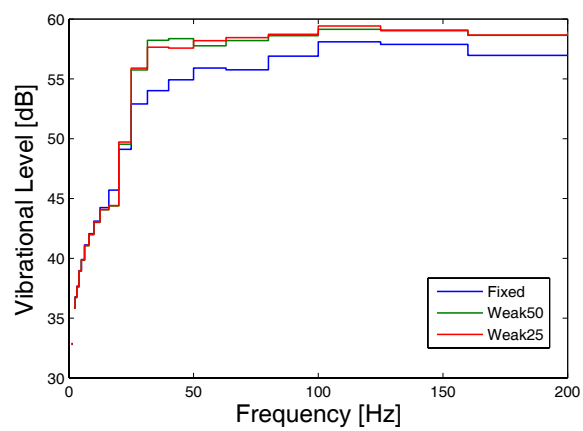

Figure 9.5: Vibrational level in apartment 1, storey 1 when excited at storey 4 for models `fixed`, `weak25` and `weak50`

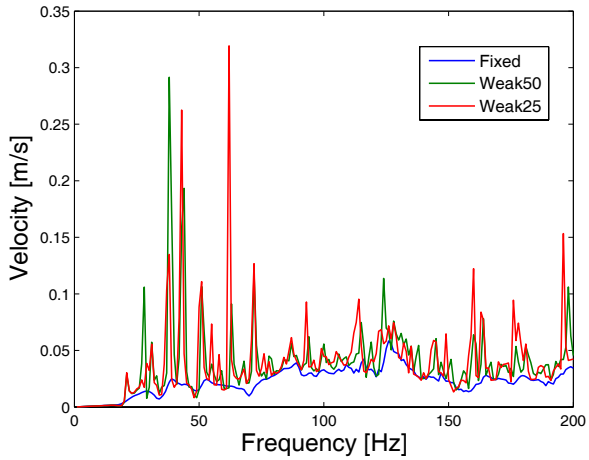

Figure 9.6: Velocity in apartment 1, storey 1 when excited at storey 4 for models `fixed`, `weak25` and `weak50`

between the lowest and middle storey was over 5 dB for `fixed`, but only around 3 dB for `weak25`. An increase of 5 dB corresponds to a velocity increase of 80 %, while a difference of 3 dB just corresponds to 40 %, this because of the logarithmic scale and the definition of vibrational level (see equation 2.1). The vibration differences are therefore more obvious in the velocity plot than in the vibrational level plot, which is noticed by comparing figure 9.7 and figure 9.8. The differences in vibrational level between the middle and the top storeys of the building were decreasing for an increasing frequency.

The velocities obtained from apartment 3 did not show the same characteristics as the ones of apartment 1: Up to 100 Hz the vibrational level was lowest further down in the building and highest on the top. The highest difference between these was 5 dB. For higher frequencies the middle and the lowest storey were showing the highest vibrational level in contrast to apartment 1 where the lowest storey always had the highest velocities and the middle the least. Here the vibrational level of the storeys differed by only about 1 dB and the result in form of the different curves was not as easy to distinguish any more. An example for the output in apartment 3 is shown in figure 9.9. When analyzing more specifically the transmission from apartment 1 to the room on the other side of the apartment separating wall (apartment 3), it

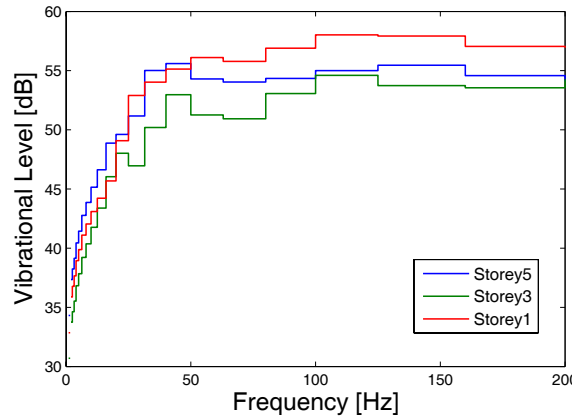

Figure 9.7: Vibrational level in apartment 1 storey 5, 3 and 1 when excited at storey 6 for model `fixed`

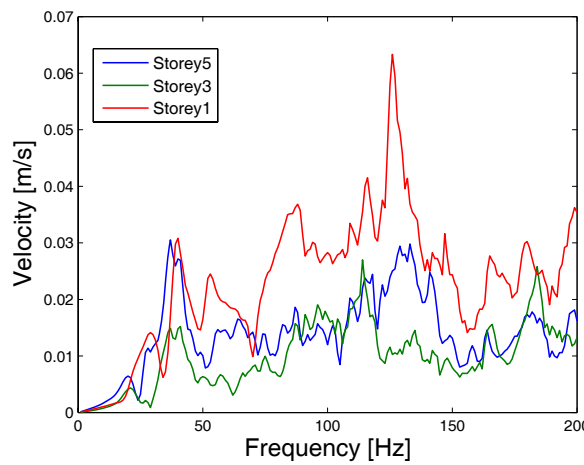

Figure 9.8: Velocities in apartment 1 storey 5, 3 and 1 when excited at storey 6 for model `fixed`

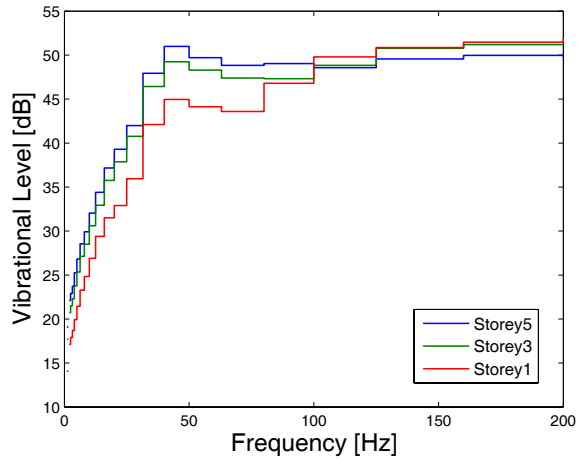

Figure 9.9: Vibrational level in apartment 3 storey 5, 3 and 1 when excited at storey 4 for model `fixed`

was observed that the lowest storey vibrated least for frequencies below 100 Hz and for higher frequencies it was the middle that vibrated least. The top story had the top velocity for all frequencies. This is shown in figure 9.10.

9.3 The influence of the storey of excitation

Another interesting observation was that it did not play any major role for the output on a certain storey whether the excitation was on storey 2, 4 or 6. This is shown in both the velocity and vibrational level plots, see figure 9.3, 9.4 and 9.11. The vibration level was thus independent on which floor the excitation was originated.

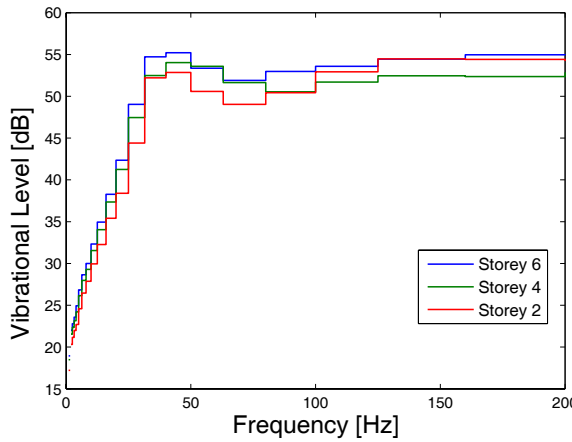

Figure 9.10: Vibrational level in apartment 3, storey 6, 4, and 2 when excited in the neighboring apartment for model `weak50`

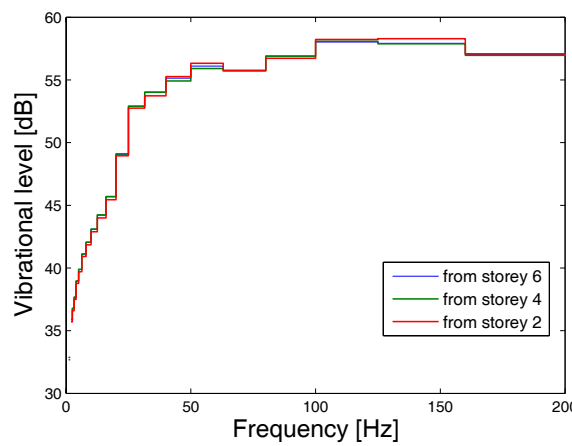

Figure 9.11: Vibrational level in apartment 1, storey 1 when excited at storey 6, 4 and 2 for model `fixed`

Chapter 10

Discussion and conclusion

The building parts were modelled by shells which were not fully able to represent all the dynamic properties as discussed in section 7.4. First of all it was difficult to find a distinct static behavior of the building parts, since they contained different materials and shapes in the different directions. This approach led to shells where the properties were averages of the stiffer regions (beams or studs). The coupled behavior and the mass distribution were not taken into consideration. Other types of stiffness analyses could have been performed to find the coupled elements of the section properties. The connections between wall and floor structure were simplified and a lot of details were not included in the model at all.

The conclusions based on the results are the following:

- The models with more flexible joints were found to have higher vibrational levels. When using weaker connections no significant difference was observed regarding how weak they were.

- Concerning the vertical vibration transmission, the lower storeys of the wood building were in general exposed to higher vibrational levels than the other storeys. The lowest vibrational levels were found in the middle of the building.

- There was not observed any general behavior concerning the diagonal transmission across the apartment separating wall. Which storey that was exposed to the highest vibrational level depended on the frequency.

- The vibration transmission between two neighboring apartments was highest at the top storeys of the building.

- At which storey the excitation point was situated was not important for the vibrational level at a specific storey.

All the above conclusions were found for the specific building at *Limnologen*. Whether they are valid for other wood buildings is still to be examined. Moreover, the analyses were only made for two chosen apartments at specific distances from the walls. Questions arise such as if the result would become different if apartment 3 had been the excitation room instead of apartment 1 or if the excitation force was positioned somewhere else on the floor. How much are the different shapes of the floor structures affecting the specific result? These questions could have been investigated but was not possible within the time frame of a master's thesis' work. Above all, the model includes a large number of simplifications which probably affect the results.

Concerning the connections between wall and floor structure the results turned out differently than first expected. Previously, we assumed that a weaker model would reduce the vibrations. The rule of thumb for step sound reduction is to use heavier floor structures and to give them weaker connections. Therefore we expected the velocity to decrease, when weaker connections are used. The exact opposite was observed in the results.

It was found that the middle storeys of the building were not exposed to as high vibrational levels as the upper and lower storeys, when investigating vertical transmission. A reasonable guess would be that vibrations also are less transmitted when the excitation is on the middle storeys. This is something that has not been confirmed by the analyses. As mentioned before it does not seem to matter significantly where the disturbance originates.

There may be several reasons why the vibrational levels of the various storeys differ from each other for vertical and horizontal transmission. One reason may be due to the type of constraint on the storeys: The highest storey is less restrained than the lowest which is closer to the ground fixations. Moreover, the weight resting on a storey is lower the higher the storey is situated in the building. The steady state response is the sum of direct, reflected waves from flanking transmission in a very complex way. How these factors are interacting has not been established in this project.

Chapter 11

Suggestions for further work

The choice of representing the floors and walls by shells, which decreased the size of the model, did not allow to entirely describe the complex dynamic behavior of the building. There are other ways of modelling complicated structures, as the earlier mentioned method of substructures. A good idea would therefore be to further develop a method of representing complex structures in dynamic analyses in a more accurate way.

During the time of the master thesis vibration measurements were performed at *Limnologen*. Since they were not designed in accordance with our analyses, direct comparison is not possible to make. There is thus a need to verify the results of the the analyses with experimental measurements.

The excitations force was applied on one special point of the floor structure at storey 2, 4 and 6. To be sure that our results are valid for the whole building, further analyses should be performed where the excitation is situated at different points of the floor structure.

Another natural continuation of this project could be to further investigate the consequences of different joints of the floor structures. One approach would be to examine what happens if the joints are not the same at different storeys.

During these analyses there was no variation of the damping in the building. It could be therefore be interesting to see whether other damping properties would influence the result.

Last but not least in future models of the building the fluid-structure interactions could be included. This would make the model more realistic and

probably the results would be more reliable.

Bibliography

[1] Bodig, J. and Jayne, B. (1982). *Mechanics of wood and wood composites*. Van Nostrand Reinhold Company Inc

[2] Brandt, O. (1958). *Akustisk planering 1*. Viktor Pettersons Bokindustri Aktiebolag

[3] Brunskog, J., Johansson, A-C. and Bahtijaragic, Z. (2006). *Svikt och vibrationer i bjälklag.* Bygg och teknik, 3/06.

[4] Chopra, A.K. (2001). *Dynamics of structures, Theory and applications to earthquake engineering*. Prentice Hall

[5] Dinwoodie J.M. (1981). *Timber, its nature and behavior*. Van Nostrand Reinhold Company

[6] Formas (2007) *Bioenergi- till vad och hur mycket?*. Forskningsrådet Formas

[7] Gustafsson P.J., (2007). *Lecture notes, Beam Theory*. Division of structural mechanics

[8] Gyproc AB, (1999). *Gyproc handbok A*.

[9] *Handbok och formelsamling i Hållfasthetslära*. Institutionen för hållfasthetslära KTH.

[10] Heiduschke, A., Kasal, B. and Haller, P. (2006). *Analyisis of wood-composite laminated frames under dynamic loads- analytical models and model validation. Part 2: frame model*. Progress in Structural Engineering and Materials, Volume **8**, 111-119.

[11] Inman, D. (2001). *Engineering vibration*. Prentice Hall.

[12] Kollmann, F. (1951). *Technologie des Holzes und der Holzwerkstoffe*. Springer Verlag Berlin

[13] Martinsons Byggsystem AB (2008). *www.martinsons.se*. Martinsons Byggsystem AB

[14] Persson, K. (2000). *Micromechanical modelling of wood and fibre properties*. Doc. Thesis, Div. of Structural Mechanics, Lund University.

[15] Ohlrich, M., Hugin, C.T. (2004). *On the influence of boundary constraints and angled baffle arrangements on sound radiation from rectangular plates.* Journal of sound and vibration, Volume **277**, 405-418.

[16] Ottosen, N. S. and Petersson, H. (1992). *Introduction to the finite element method*. Prentice Hall

[17] Simula (2007). *Abaqus version 6.7 documentation*.

[18] Soedel, W. (2004). *Vibrations of shells and plates*. New York Marcel Dekker cop.

[19] Träguiden (2008). *www.traguiden.se, internet based documents about wood*. Sveriges Skogsindustrier